Structural capacity assessment of PC members subjected to different corrosion-induced damage scenarios

Beatrice Belletti, University of Parma, Italy

CONTENTS

Presentation based on the Key – note presented at the fib Symposium 2025 in Antibes

INTRODUCTION

The Corrosion Phenomenon: Background and Developments

- In the past century, the prestressing construction technique has been widely used and nowadays several structures and infrastructures are beyond their service life.

- Mainly due to **lack of maintenance**, a significant part of existing bridges is subjected to deterioration phenomena induced by corrosion.

R = [H] x [E] x [V]

The risk of durability issues increases over the time.

Hazard (H)

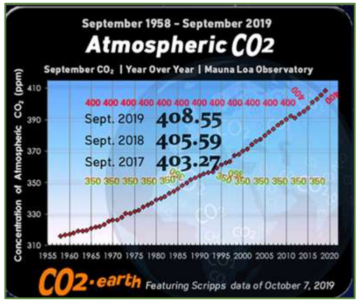

Vulnerability (V)

Ref. Linee guida per la classificazione e gestione del rischio, la valutazione della sicurezza ed il monitoraggio dei ponti esistenti. 2022

Exposition (E)

Ref. Making Critical Infrastructure Resilient, 2020 UNDRR, Shutterstock, Unsplash

Italian Guidelines

In several countries, guidelines for bridges management propose defect-based index to provide a qualitative measure of bridge vulnerability.

Italian Guidelines

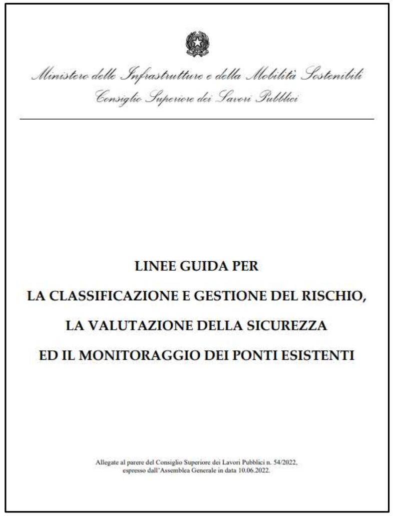

Multi-level approach

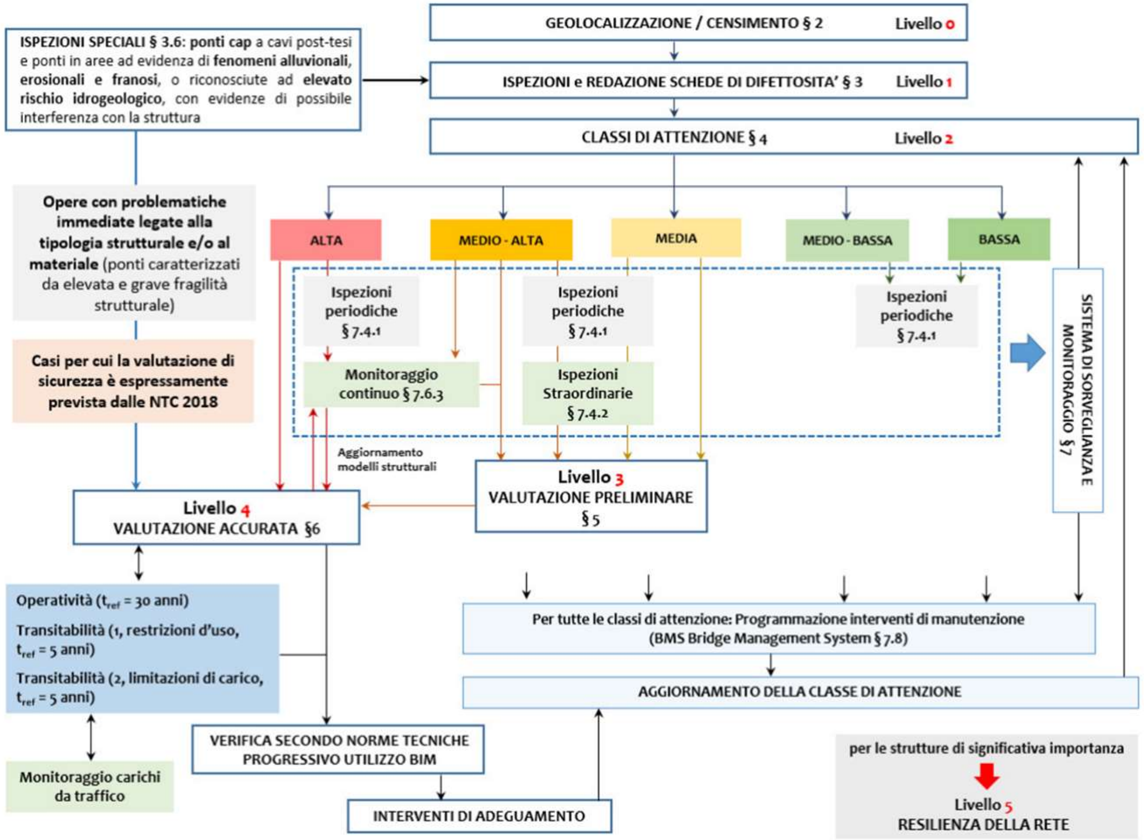

MIT, "DM. 01 July 2022. Guidelines for the classification and risk Management, safety assessment and monitoring of existing bridges," Italian High Council of Public Works (in italian), 2022

Level1
- According to practices adopted during visual inspections, corrosion levels are defined in terms of extension and intensity

Level 2
- Classification of the level of deterioration
- The classification of the level of deterioration reached in each component is finally obtained after combining the gravity attribute to the noted defects, together with their extension and intensity levels

Level 3
- Load analysis and comparisons of demand calculated according to the actual traffic load values and the traffic load values adopted for the original design

Level 4
- Higher accuracy in the measurement of the corrosion level can be achieved, after accurate inspections, useful also for the assessment of the bridge safety according to Level 4 and via numerical calculations

Visual inspection: Level 1

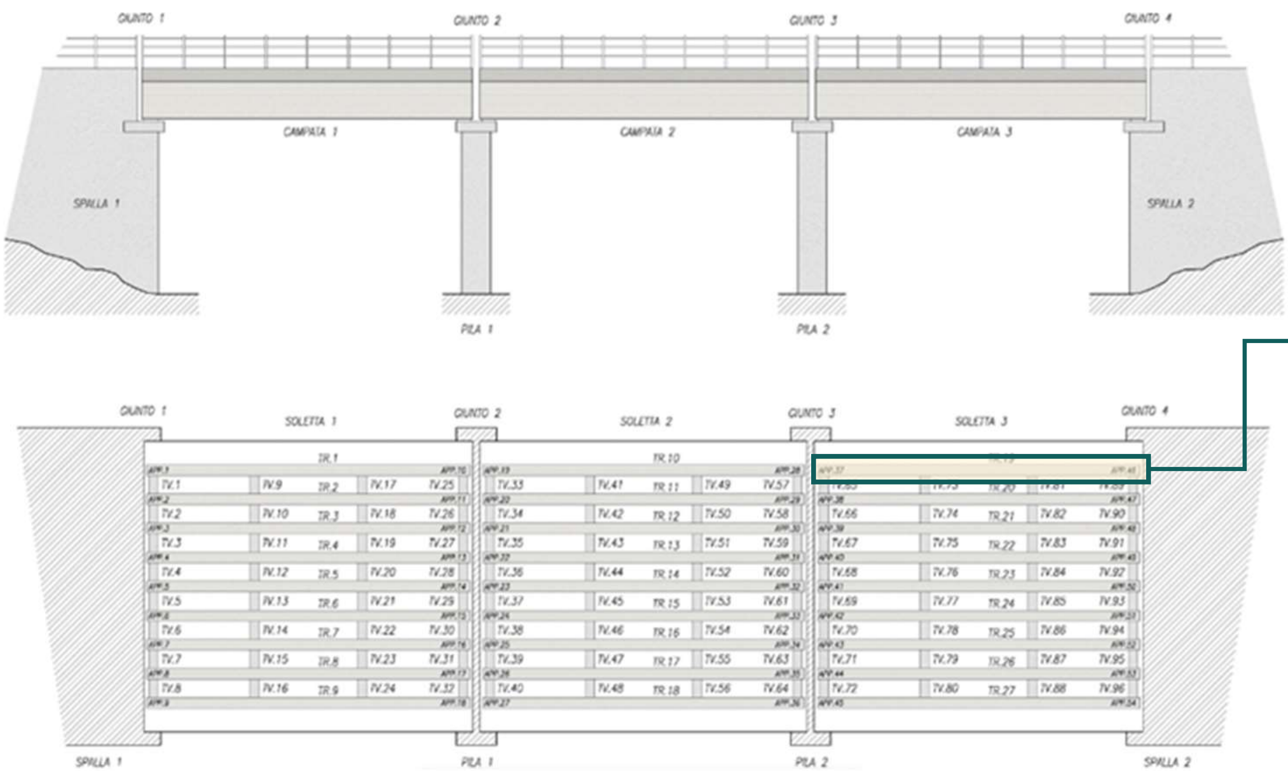

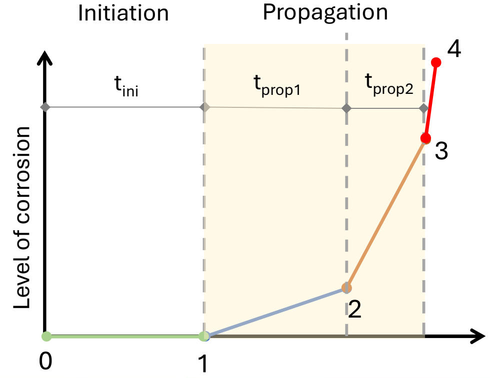

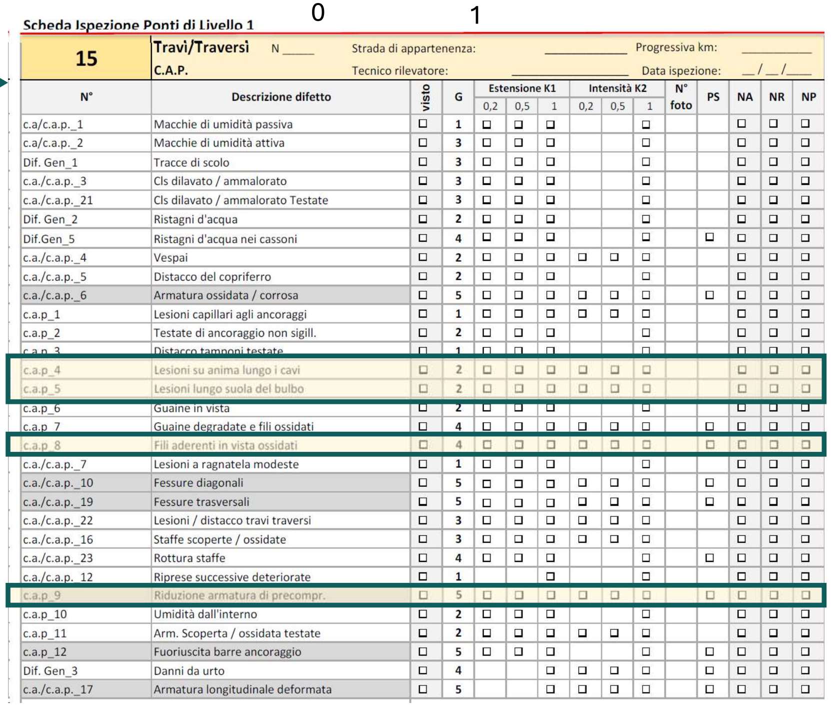

Scheda Ispezione Ponti di Livello 1

15 | **Travi/Traversi** N ____ **C.A.P.** | Strada di appartenenza: ____________ Progressiva km: ____________ | Tecnico rilevatore: ____________ Data ispezione: __/__/____

N°	Descrizione difetto	visto	G	Estensione K1			Intensità K2			N° foto	PS	NA	NR	NP
				0,2	0,5	1	0,2	0,5	1					
c.a/c.a.p._1	Macchie di umidità passiva	☐	1	☐	☐	☐			☐			☐	☐	☐
c.a/c.a.p._2	Macchie di umidità attiva	☐	3	☐	☐	☐			☐			☐	☐	☐
Dif. Gen_1	Tracce di scolo	☐	3	☐	☐	☐			☐			☐	☐	☐
c.a./c.a.p._3	Cls dilavato / ammalorato	☐	3	☐	☐	☐			☐			☐	☐	☐
c.a./c.a.p._21	Cls dilavato / ammalorato Testate	☐	3	☐	☐	☐			☐			☐	☐	☐
Dif. Gen_2	Ristagni d'acqua	☐	2	☐	☐	☐			☐			☐	☐	☐
Dif.Gen_5	Ristagni d'acqua nei cassoni	☐	4	☐	☐	☐			☐		☐	☐	☐	☐
c.a./c.a.p._4	Vespai	☐	2	☐	☐	☐	☐	☐	☐			☐	☐	☐
c.a./c.a.p._5	Distacco del copriferro	☐	2	☐	☐	☐			☐			☐	☐	☐
c.a./c.a.p._6	Armatura ossidata / corrosa	☐	5	☐	☐	☐	☐	☐	☐		☐	☐	☐	☐
c.a.p_1	Lesioni capillari agli ancoraggi	☐	1	☐	☐	☐	☐	☐	☐			☐	☐	☐
c.a.p_2	Testate di ancoraggio non sigill.	☐	2	☐	☐	☐			☐			☐	☐	☐
c.a.p_3	Distacco tamponi testate	☐	1	☐	☐	☐			☐			☐	☐	☐
c.a.p_4	Lesioni su anima lungo i cavi	☐	2	☐	☐	☐	☐	☐	☐			☐	☐	☐
c.a.p_5	Lesioni lungo suola del bulbo	☐	2	☐	☐	☐	☐	☐	☐			☐	☐	☐
c.a.p_6	Guaine in vista	☐	2	☐	☐	☐			☐			☐	☐	☐
c.a.p_7	Guaine degradate e fili ossidati	☐	4	☐	☐	☐	☐	☐	☐		☐	☐	☐	☐
c.a.p_8	Fili aderenti in vista ossidati	☐	4	☐	☐	☐	☐	☐	☐		☐	☐	☐	☐
c.a./c.a.p._7	Lesioni a ragnatela modeste	☐	1	☐	☐	☐			☐			☐	☐	☐
c.a./c.a.p._10	Fessure diagonali	☐	5	☐	☐	☐	☐	☐	☐		☐	☐	☐	☐
c.a./c.a.p._19	Fessure trasversali	☐	5	☐	☐	☐	☐	☐	☐		☐	☐	☐	☐
c.a./c.a.p._22	Lesioni / distacco travi traversi	☐	3	☐	☐	☐	☐	☐	☐			☐	☐	☐
c.a./c.a.p._16	Staffe scoperte / ossidate	☐	3	☐	☐	☐	☐	☐	☐			☐	☐	☐
c.a./c.a.p._23	Rottura staffe	☐	4	☐	☐	☐			☐		☐	☐	☐	☐
c.a./c.a.p._12	Riprese successive deteriorate	☐	1			☐			☐			☐	☐	☐
c.a.p_9	Riduzione armatura di precompr.	☐	5	☐	☐	☐	☐	☐	☐		☐	☐	☐	☐
c.a.p_10	Umidità dall'interno	☐	2	☐	☐	☐			☐			☐	☐	☐
c.a.p_11	Arm. Scoperta / ossidata testate	☐	2	☐	☐	☐	☐	☐	☐			☐	☐	☐
c.a.p_12	Fuoriuscita barre ancoraggio	☐	5	☐	☐	☐			☐		☐	☐	☐	☐
Dif. Gen_3	Danni da urto	☐	4			☐	☐	☐	☐		☐	☐	☐	☐
c.a./c.a.p._17	Armatura longitudinale deformata	☐	5			☐	☐	☐	☐		☐	☐	☐	☐

- According to practices adopted during visual inspections, corrosion levels are defined in terms of extension and intensity.
- The classification of the level of deterioration reached in each component is finally obtained after combining the gravity attribute to the noted defects, together with their extension and intensity levels.

Visual inspection: Level 1

Scheda Ispezione Ponti di Livello 1

15	**Travi/Traversi** C.A.P.	N _____	Strada di appartenenza: ____________	Progressiva km: __________
			Tecnico rilevatore: ________________	Data ispezione: __/__/____

N°	Descrizione difetto	visto	G	Estensione K1 0,2	Estensione K1 0,5	Estensione K1 1	Intensità K2 0,2	Intensità K2 0,5	Intensità K2 1	N° foto	PS	NA	NR	NP
c.a/c.a.p._1	Macchie di umidità passiva	☐	1	☐	☐	☐			☐			☐	☐	☐
c.a/c.a.p._2	Macchie di umidità attiva	☐	3	☐	☐	☐			☐			☐	☐	☐
Dif. Gen_1	Tracce di scolo	☐	3	☐	☐	☐			☐			☐	☐	☐
c.a./c.a.p._3	Cls dilavato / ammalorato	☐	3	☐	☐	☐			☐			☐	☐	☐
c.a./c.a.p._21	Cls dilavato / ammalorato Testate	☐	3	☐	☐	☐			☐			☐	☐	☐
Dif. Gen_2	Ristagni d'acqua	☐	2	☐	☐	☐			☐			☐	☐	☐
Dif.Gen_5	Ristagni d'acqua nei cassoni	☐	4	☐	☐	☐			☐		☐	☐	☐	☐
c.a./c.a.p._4	Vespai	☐	2	☐	☐	☐	☐	☐	☐			☐	☐	☐
c.a./c.a.p._5	Distacco del copriferro	☐	2	☐	☐	☐			☐			☐	☐	☐
c.a./c.a.p._6	Armatura ossidata / corrosa	☐	5	☐	☐	☐	☐	☐	☐		☐	☐	☐	☐
c.a.p_1	Lesioni capillari agli ancoraggi	☐	1	☐	☐	☐	☐	☐	☐			☐	☐	☐
c.a.p_2	Testate di ancoraggio non sigill.	☐	2	☐	☐	☐			☐			☐	☐	☐
c.a.p_3	Distacco tamponi testate	☐	1	☐	☐	☐			☐			☐	☐	☐
c.a.p_4	Lesioni su anima lungo i cavi	☐	2	☐	☐	☐	☐	☐	☐			☐	☐	☐
c.a.p_5	Lesioni lungo suola del bulbo	☐	2	☐	☐	☐	☐	☐	☐			☐	☐	☐
c.a.p_6	Guaine in vista	☐	2	☐	☐	☐			☐			☐	☐	☐
c.a.p_7	Guaine degradate e fili ossidati	☐	4	☐	☐	☐	☐	☐	☐		☐	☐	☐	☐
c.a.p_8	Fili aderenti in vista ossidati	☐	4	☐	☐	☐	☐	☐	☐		☐	☐	☐	☐
c.a./c.a.p._7	Lesioni a ragnatela modeste	☐	1	☐	☐	☐			☐			☐	☐	☐
c.a./c.a.p._10	Fessure diagonali	☐	5	☐	☐	☐	☐	☐	☐		☐	☐	☐	☐
c.a./c.a.p._19	Fessure trasversali	☐	5	☐	☐	☐	☐	☐	☐		☐	☐	☐	☐
c.a./c.a.p._22	Lesioni / distacco travi traversi	☐	3	☐	☐	☐	☐	☐	☐			☐	☐	☐
c.a./c.a.p._16	Staffe scoperte / ossidate	☐	3	☐	☐	☐	☐	☐	☐			☐	☐	☐
c.a./c.a.p._23	Rottura staffe	☐	4	☐	☐	☐			☐		☐	☐	☐	☐
c.a./c.a.p._12	Riprese successive deteriorate	☐	1			☐			☐			☐	☐	☐
c.a.p_9	Riduzione armatura di precompr.	☐	5	☐	☐	☐	☐	☐	☐		☐	☐	☐	☐
c.a.p_10	Umidità dall'interno	☐	2	☐	☐	☐			☐			☐	☐	☐
c.a.p_11	Arm. Scoperta / ossidata testate	☐	2	☐	☐	☐	☐	☐	☐			☐	☐	☐
c.a.p_12	Fuoriuscita barre ancoraggio	☐	5	☐	☐	☐			☐		☐	☐	☐	☐
Dif. Gen_3	Danni da urto	☐	4			☐	☐	☐	☐		☐	☐	☐	☐
c.a./c.a.p._17	Armatura longitudinale deformata	☐	5			☐	☐	☐	☐		☐	☐	☐	☐

Schede difettologiche **N° difetto: c.a./c.a.p._2**

Macchie di umidità attiva

Peso del difetto

G = 1 | G = 2 | **G = 3** | G = 4 | G = 5

Estensione k_1	0,2 (appena presente)	0,5 (~50% superficie)	1 (~tutta la superficie)
Intensità k_2	Sempre = 1		

Descrizione

Il difetto si presenta con aree di colorazione diversa dal materiale integro. In particolare, si tratta di tracce di calcio rilasciate sulla superficie dall'umidità penetrata attraverso il calcestruzzo. A differenza delle macchie di umidità passiva, l'**umidità attiva** è legata a fenomeni di infiltrazione di acqua tutt'ora in corso e si presenta con macchie di colore scuro dovuto al contatto continuo con l'acqua e l'umidità.

Cause

La penetrazione di umidità e di acqua meteorica attraverso i
presenza di:

- materiali caratterizzati da elevata porosità;
- mancanza o carenze nel sistema di impermeabilizzazione;
- sistemi di convogliamento delle acque assenti, inadeguati
- imperfetta tenuta dei giunti;
- scossaline assenti o deteriorate.

Fenomeni di degrado correlati

Il progredire di tale fenomeno di degrado potrebbe cor **fenomeni di dilavamento e di ammaloramento** del calces **distacchi di copriferro** con conseguente esposizione delle a diverso da altri fenomeni, quali le **tracce di scolo**, dovuti a s acqua.

Lesioni lungo suola del bulbo

Peso del difetto

G = 1 | **G = 2** | G = 3 | G = 4 | G = 5

Estensione k_1	0,2 (appena presente)	0,5 (~50% superficie)	1 (~tutta la superficie)
Intensità k_2	0,2 (In media < 1)	0,5 (In media da 1 a 3)	1 (In media > 3)

Descrizione

Il difetto si riferisce alla presenza di fessure, nella direzione longitudinale delle travi in c.a.p. a cavi scorrevoli, che seguono l'andamento di questi ultimi. Generalmente sono più frequenti in corrispondenza della mezzeria delle travi e sono spesso accompagnate da macchie di umidità, che rendono più semplice il loro rilevamento. Il difetto comprende anche le lesioni all'intradosso di solettoni, cassoni e archi in c.a.p.

Cause

La presenza di fessure deriva, innanzitutto, dalla presenza di uno strato di ricoprimento in calcestruzzo delle guaine non adeguato; in tal caso, esso può esser facilmente fessurato nel caso in cui le guaine metalliche, ossidandosi, aumentano di volume. Il fenomeno è accentuato in presenza di acqua all'interno delle guaine e non completa o mancata iniezione delle stesse.

Fenomeni di degrado correlati

Tale tipologia di lesione non deve essere confusa con gli altri stati fessurativi, che non dipendono dalla presenza delle guaine. L'evoluzione del fenomeno può far insorgere ulteriori difetti, quali **guaine in vista** e **guaine degradate**.

Fonte: PROGETTO RAM – Manuale c GRUPPO FS ITA

Schede difettologiche **N° difetto: c.a.p._8**

Fili aderenti in vista ossidati

Peso del difetto

G = 1 | G = 2 | G = 3 | **G = 4** | G = 5

Estensione k_1	0,2 (appena presente)	0,5 (~50% superficie)	1 (~tutta la superficie)
Intensità k_2	0,2 (ossidata)	0,5 (Intaccata la sezione del filo)	1 (Corrosa con diminuz. di sezione)

Descrizione

Il difetto si riferisce all'esposizione dell'armatura di precompressione di elementi in c.a.p. a *cavi aderenti* e alla loro conseguente ossidazione.

Fonte: PROGETTO RAM – Manuale di ispezione principale (Anas GRUPPO FS ITALIANE)

Cause

L'ossidazione delle armature è evidente nel caso di distacco di calcestruzzo, laddove esso sia particolarmente ammalorato a causa dell'azione erosiva delle acque meteoriche. Il distacco di copriferro e la conseguente esposizione dell'armatura è più probabile nel caso di materiale di scarsa qualità.

Fonte: PROGETTO RAM – Manuale di ispezione principale (Anas GRUPPO FS ITALIANE)

Fenomeni di degrado correlati

Il fenomeno si concentra in corrispondenza di zone di **calcestruzzo dilavato/ammalorato**. La sua evoluzione può causare la corrosione dei fili e quindi la **riduzione dell'armatura di precompressione**.

Per le caratteristiche stesse della tecnologia di precompressione a cavi aderenti, tale difetto si manifesta raramente, salvo situazioni particolari.

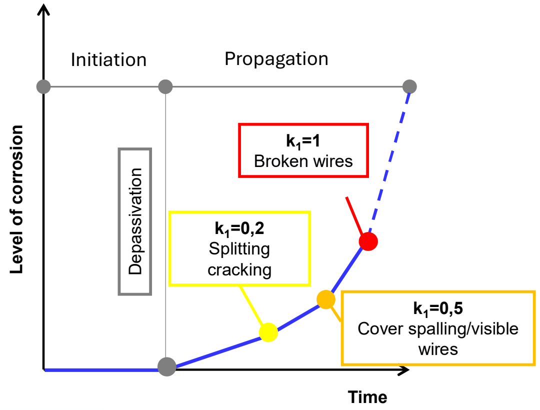

- Cracking and surface damage induced by corrosion are not differentiated from cracking induced by rheological phenomena, loads, etc.

- It results that the same defect - <u>that is in this presentation is related to the corrosion of pre-tensioned strands or wires placed in the bottom flange of the cross section</u> - at different phases of propagation could be described, during the visual inspection, by noting different types of defects.

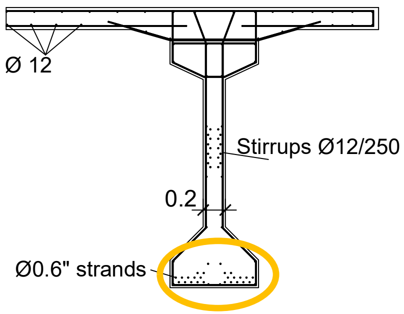

Cascading effects form Level 1

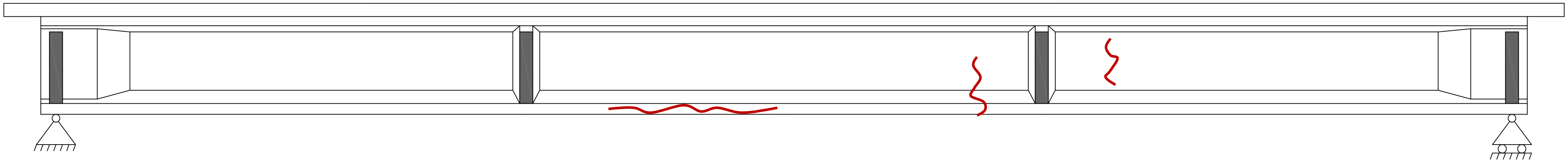

Corrosion induced defects need different actions than other defects in terms of:

- in-situ measurement related to the initiation phase (such as chloride content profile, carbonation depth, cover thickness) and propagation phase, such as electrochemical measurements (potential corrosion mapping, E_{corr}, corrosion rate, i_{corr}, resistivity, etc), surface damage mapping (opening widths of splitting cracks, w, cover spalling), cross section loss in bars, pith depth, etc.
- frequency of bridge's inspections
- modelling strategies to be adopted in Level 4
- planning of proactive and reactive repairing interventions
- Etc.

Improving the capability of defect's detection in Level 1 could allow to save time and money in further steps required for the bridge management and could allow to optimise the maintenance process

Proposal of a defect-based index suitable for the multi-level approach

Level 1 - Level 2
Based on visual inspection

Level 4
Based on structural assessment

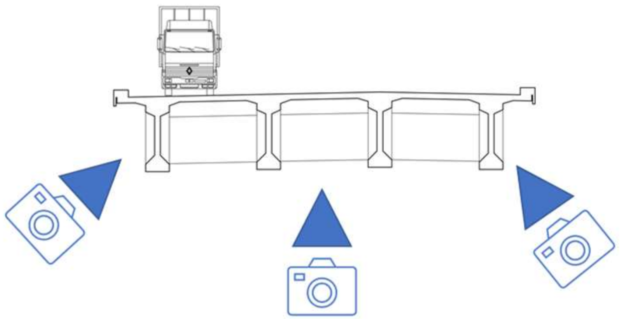

Intensity level, k_{int},
Extension level, k_{ext}

$$\boxed{\left(1 - k_{int,2} \cdot k_{ext}\right)}$$

$M_{R,\ corroded} = f(M_{R,uncorroded}, (1 - k_{int,2} \cdot k_{ext}))$

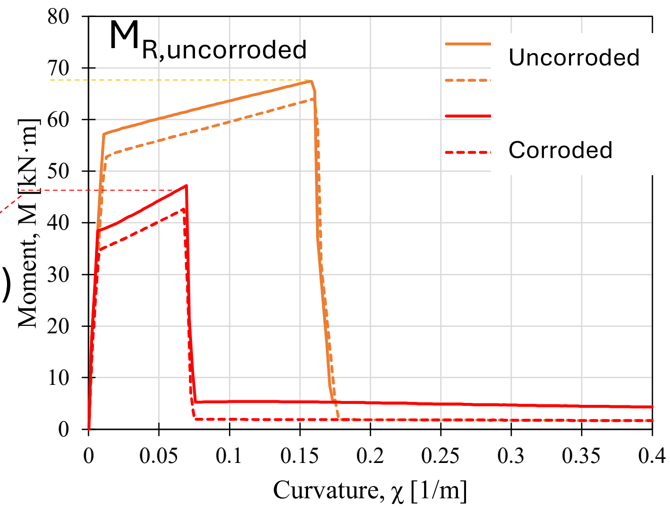

SOME NOTES:

- The parameters adopted to identify the extension and the intensity levels of corrosion in prestressing strands during visual inspections (Level 1) should be coherent and suitable also for applications of analytical and numerical models in Level 4
- The proposed procedure allows to assign a severity to the defect-based index after visual inspections – according to Level 1 and Level 2 - based on the same engineering criteria adopted during numerical assessment - in Level 4 - to account for the effects of corrosion
- Only the dependency of the flexural capacity on the extension and intensity of corrosion in prestressing strands is evaluated in this presentation

THE CASE STUDY:

A PC GIRDER OF AN EXISTING BRIDGE DECK

The Case Study: a PC girder of an Existing Bridge Deck

Location of the case study viaduct

Gallo, P.C. and Petrangeli, M.P. 1983. The viaduct crossing of the Calabria divide between Gioiosa Jonica and Rosarno. *Industria Italiana del Cemento* 53, pp. 309–332.

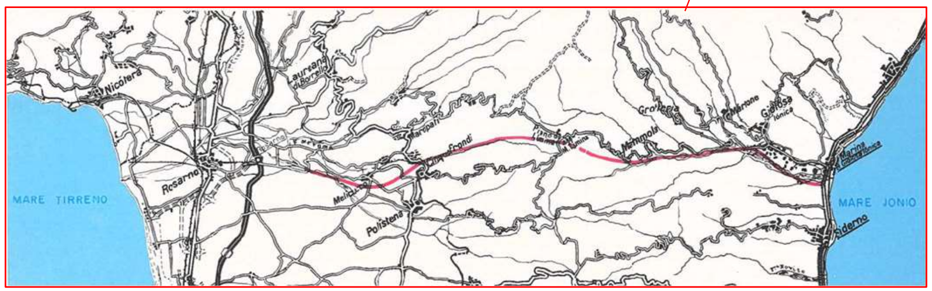

Viaduct designed in 1976 and executed in 1988

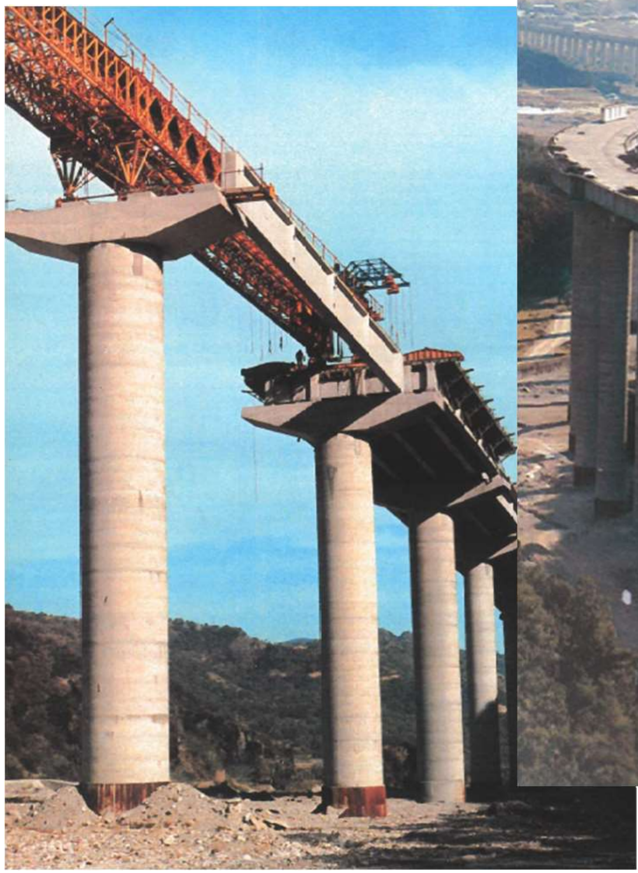

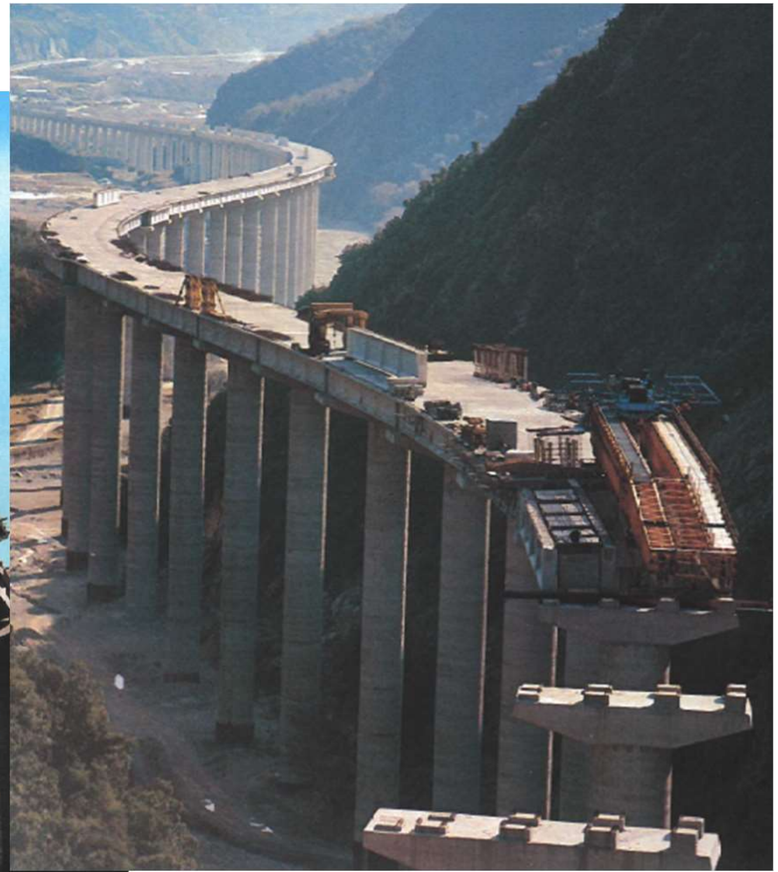

The Case Study: a PC girder of an Existing Bridge Deck

Geometrical and mechanical features

Gallo, P.C. and Petrangeli, M.P. 1983. The viaduct crossing of the Calabria divide between Gioiosa Jonica and Rosarno. *Industria Italiana del Cemento* 53, pp. 309–332.

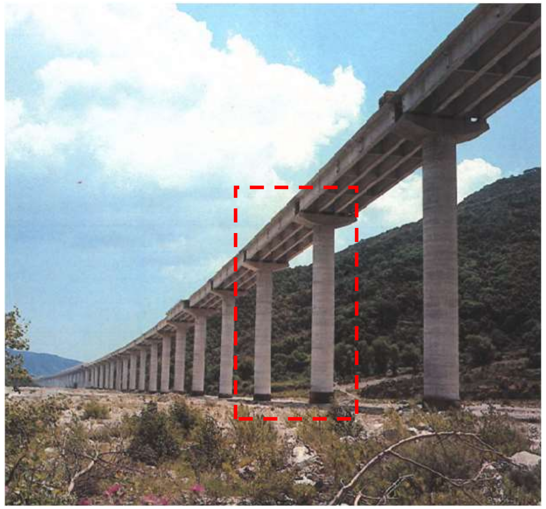

PC girder with pre-tensioned 7-wire strands

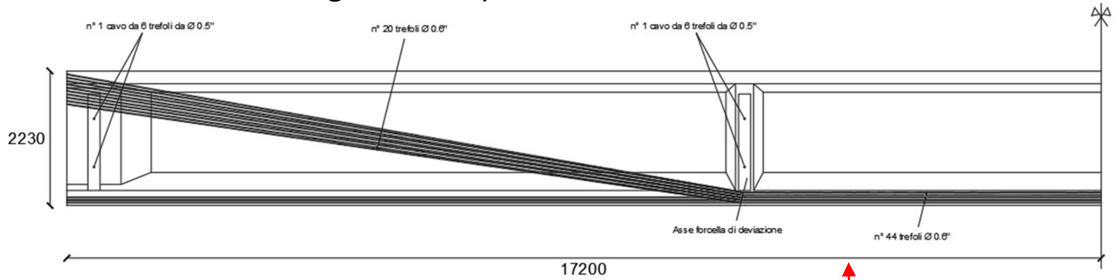

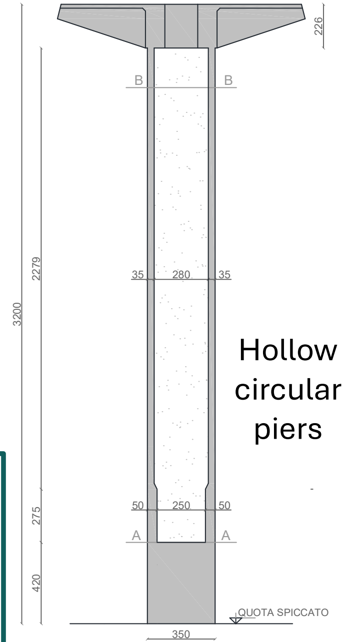

Hollow circular piers

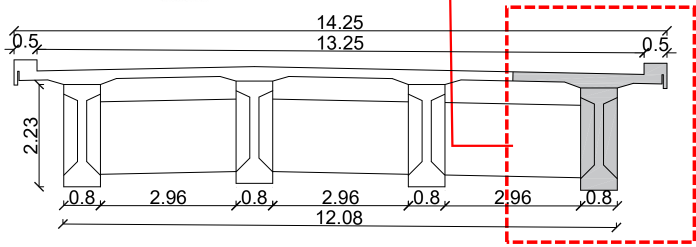

Bridge deck with simply supported beams

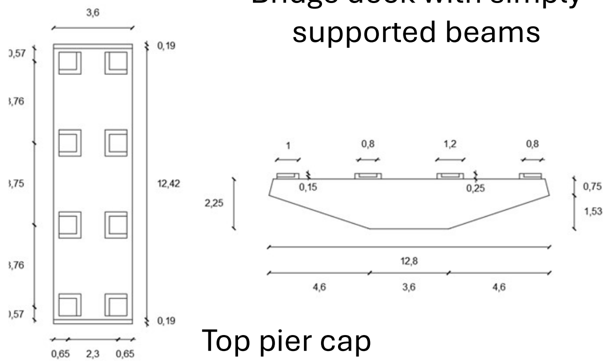

Top pier cap

In this work, corrosion scenarios are assumed and applied to the selected case study **without any reference to the actual situation of the viaduct**, which is unknown to Authors. Therefore, the selected case study represents only an example for the application of a general procedure that Authors are presenting for prestressed bridge girders.

The Case Study: a PC girder of an Existing Bridge Deck

Geometrical and mechanical features

Gallo, P.C. and Petrangeli, M.P. 1983. The viaduct crossing of the Calabria divide between Gioiosa Jonica and Rosarno. *Industria Italiana del Cemento* 53, pp. 309–332.

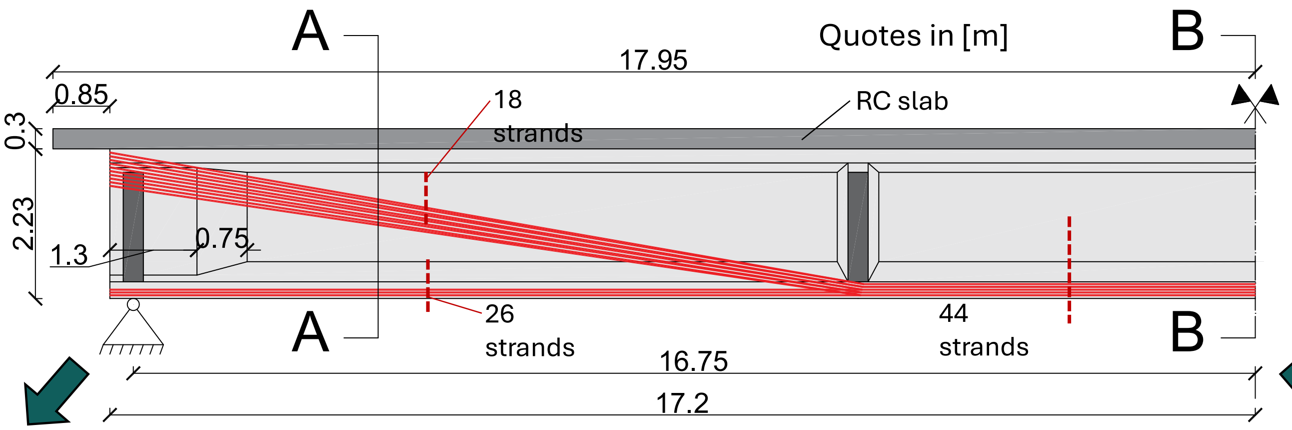

PC girder with pre-tensioned 7-wire strands:

- Simply supported PC girders
- Span Length L =34.4 m
- Height of PC beam: 2.23 m.
- RC slab thickness: 30 cm.

Section A-A

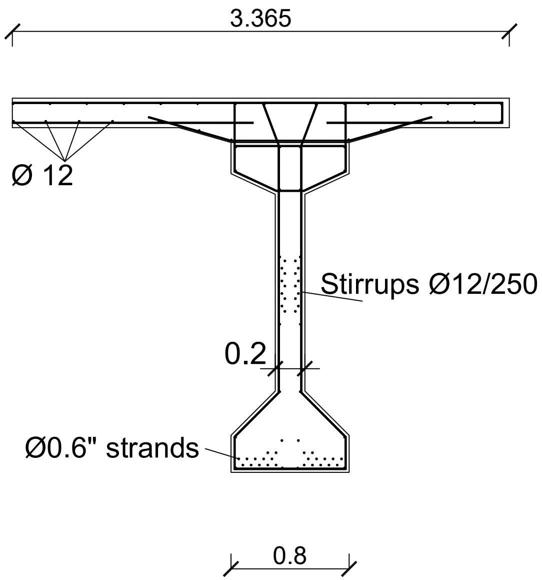

Material properties

Material	***Parameter***	***Value***
Concrete PC beam	$f_{ck,cube}$ [MPa]:	45
Concrete RC slab		35
Mild reinforcement	f_{yk} [MPa]:	430
	ε_u [-]:	0.135
Prestressing strands	$f_{p0.1k}$ [MPa]:	1670
	f_{ptk} [MPa]:	1860
	ε_{pu} [-]:	0.05

Section B-B

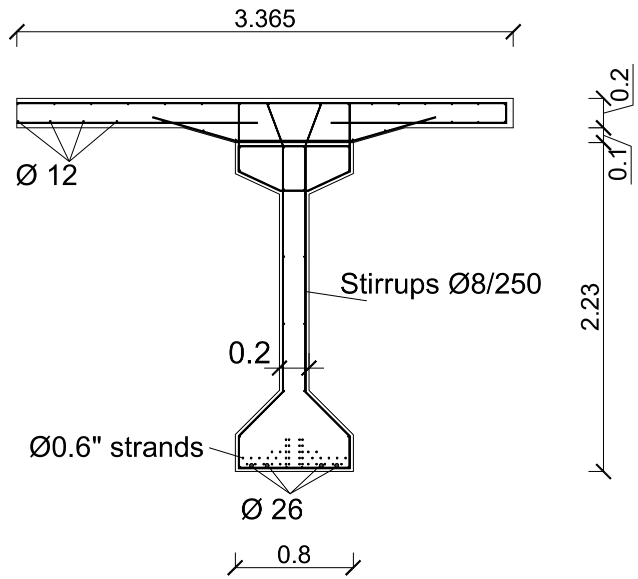

THE CORROSION MORPHOLOGY AND THE SCPS MODEL

Measuring the damage in corroded prestressing strands

“DIRECT MEASURE OF THE DEFECT”

pit depth

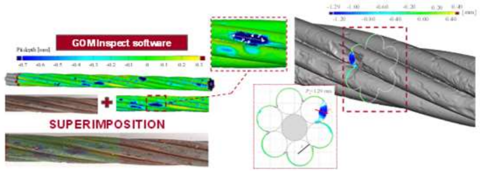

In-situ Inspection

by using a
pit depth gauge instrument

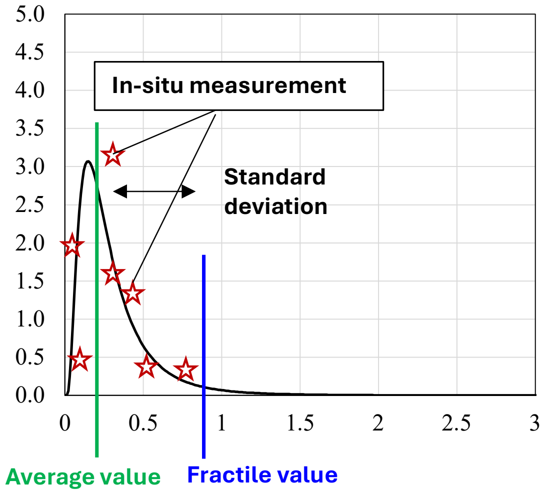

Lognormal distribution: It is possible to determine the average penetration depth and the related maximum penetration depth (Fractile value)

“INDIRECT MEASURE OF THE DEFECT”

crack width/superficial deterioration

$$w = \frac{1}{N}\sum_{j=1}^{N}\frac{\left(\sum_{i=1}^{m} w_n\right)}{m}$$

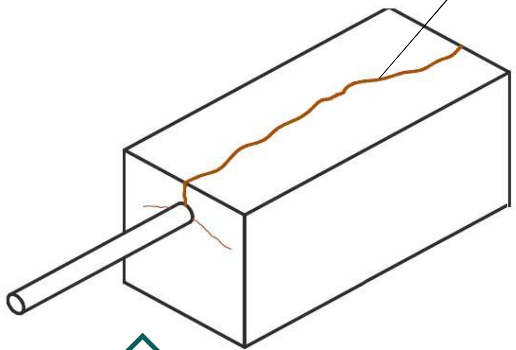

Starting from the observation of the superficial deterioration, some assumptions about the pit depth values have been made

Collecting data about the damage in corroded prestressing strands helps to interpret the measured data in-situ

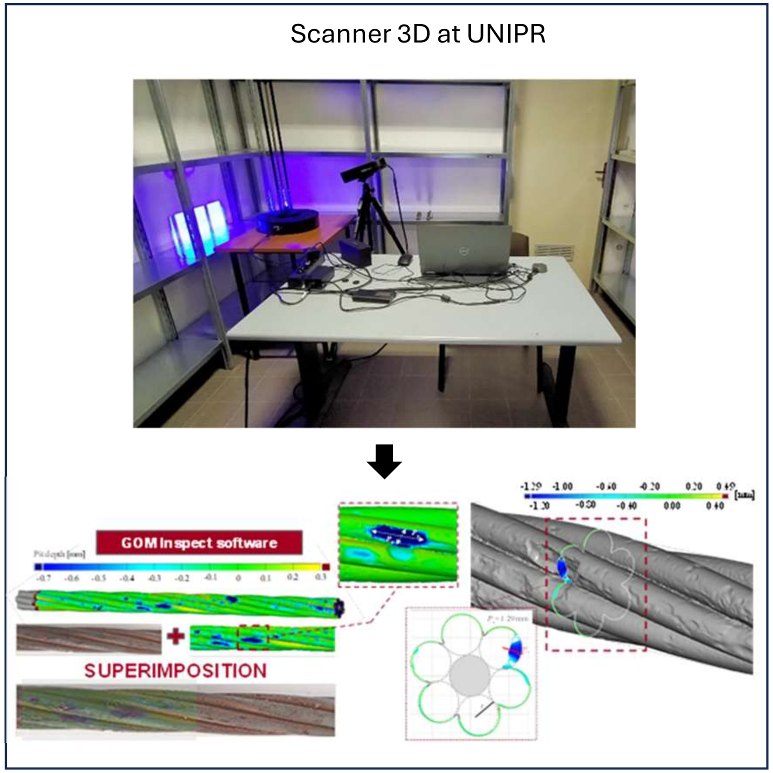

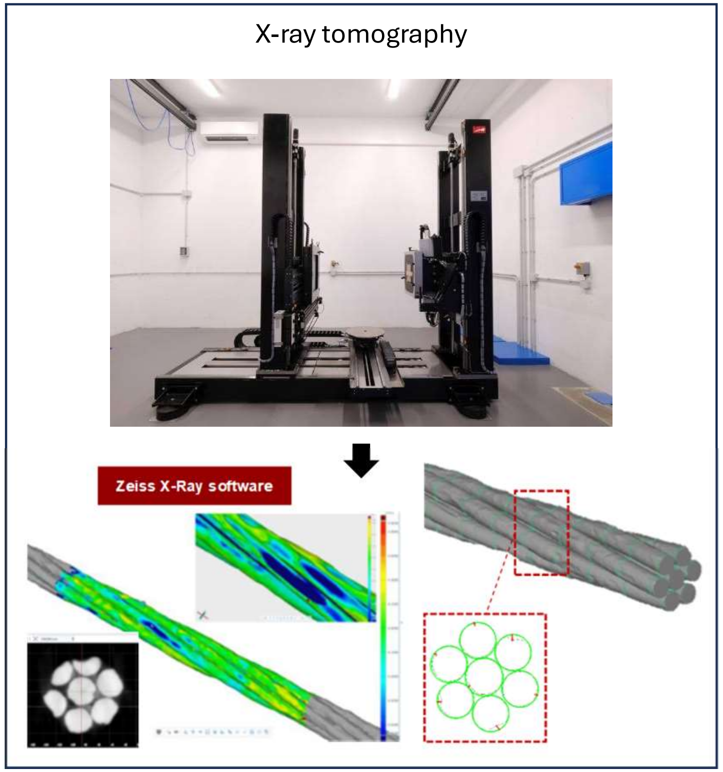

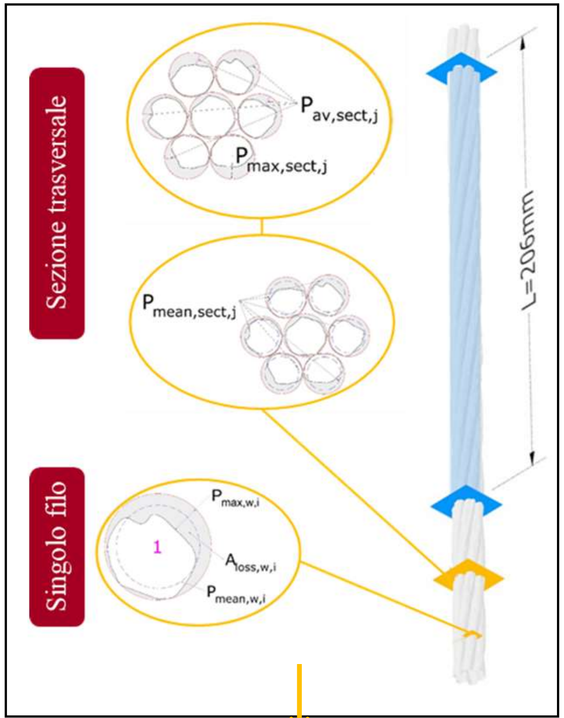

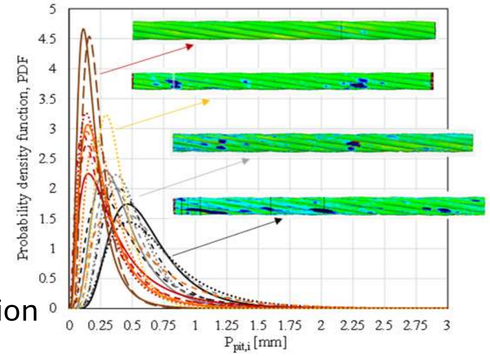

Statistical distribution

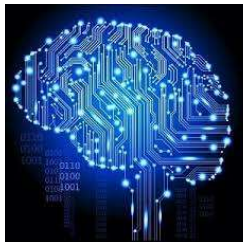

- TO DEFINE MODEL UNCERTANTIES
- TO APPLY MACHIN LEARNING TECHNIQUES
- TO MANAGE MONITORING DATA
- ETC.

The fib DATABASE on corroded strands

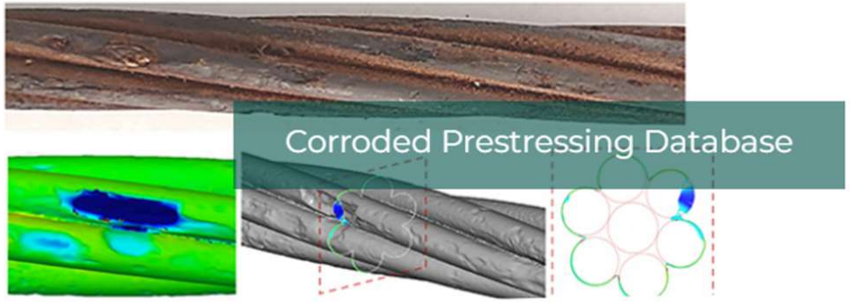

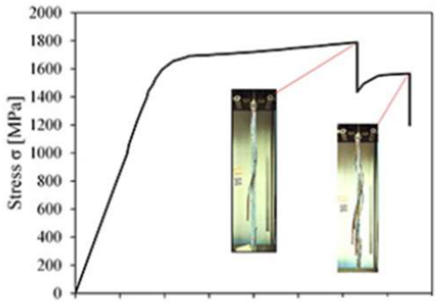

Important to collect and extend the current data

fib DATABASE

The database on the mechanical performance of corroded prestressing strands gathers data from experimental tensile tests carried out across the world. The database encompasses: (1) the corrosion type, natural or artificial, (2) the geometry and uncorroded mechanical properties, (3) the mechanical properties and the corrosion morphology and (4) the mechanical behaviour results from tests on corroded samples. In case of natural corrosion, additional information can be provided concerning the prestressed concrete members from which the samples are retrieved and environmental conditions. The database aims to provide researchers extensive data for model validation and calibrations concerning degraded prestressed concrete structures.

First public release: Feb. 2024

Database Editor
Beatrice Belletti (University of Parma, Italy)

Database Co-Editor
Simone Ravasini (University of Parma, Italy)

https://www.fib-international.org/commissions/databases.html

Measuring the damage in corroded prestressing strands

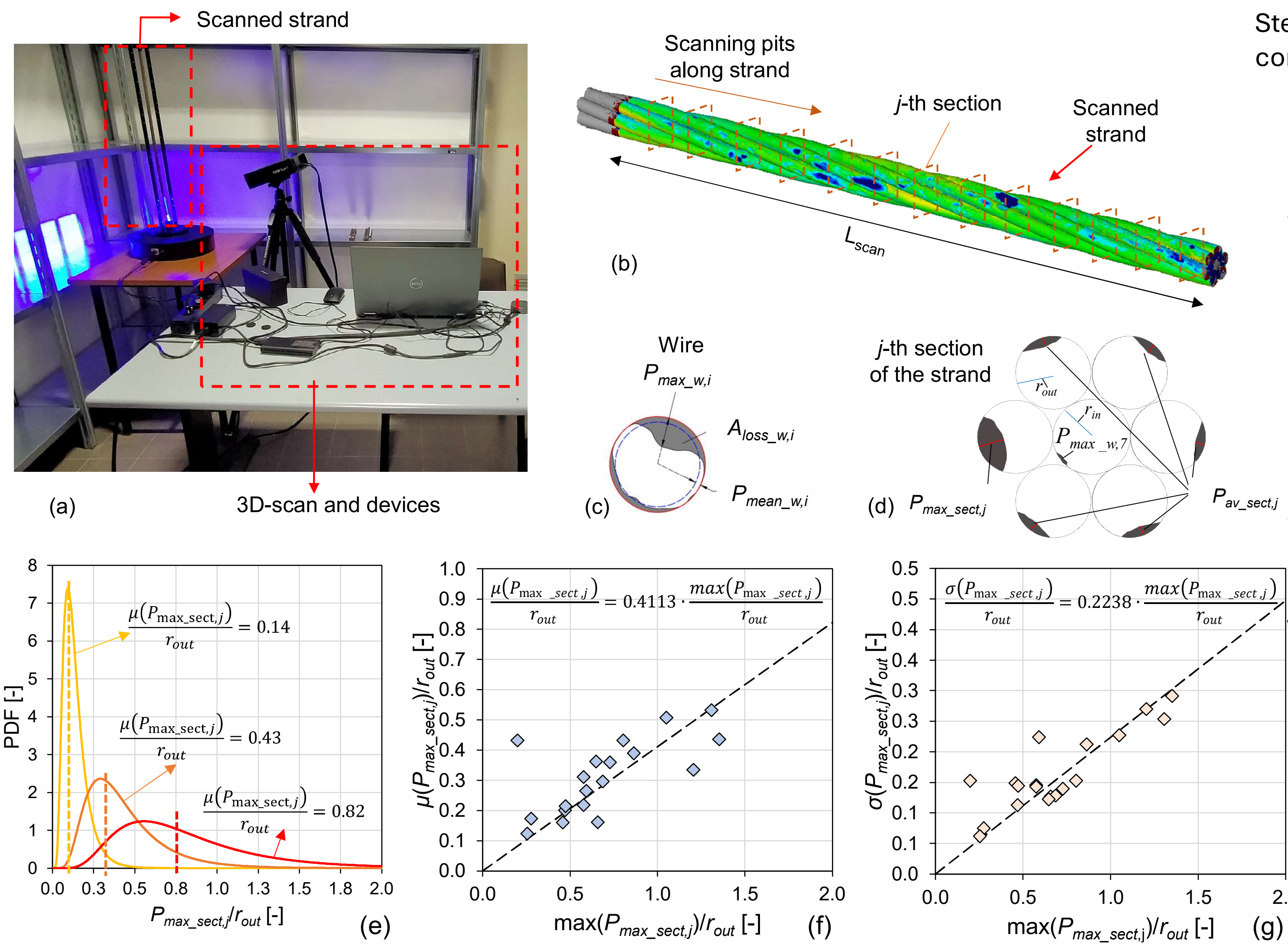

Steps for the probabilistic distribution of the corrosion morphology obtained from the 3D-scan:

1) The 3D-scan is performed, and for each strand, several cross sections - 10 mm spaced - are identified;
2) At each j-th cross section - 10 mm spaced - the maximum pit depth of each external wire, $P_{max\_w,i}$, is measured, and the maximum pit depth of the most corroded wire at the j-th section is identified as $P_{max\_sect,j}=max(P_{max\_w,i})i=1,6$. The ratio $P_{max\_sect,j}/r_{out}$, is the input parameter of the SCPS model (used for Level 4), for the assessment of the tensile capacity of corroded strands at the j-th cross section;
3) The maximum value of the variable $P_{max\_sect,j}/r_{out}$, measured along the entire length of the strand, is calculated as $P_{max,p}/r_{out} = max(P_{max\_sect,j})/r_{out}$
4) The probability density function of the variable $P_{max\_sect,j}/r_{out}$, is plotted. The mean value, $\mu(P_{max\_sect,j})/r_{out}$, and the standard deviation value, $\sigma(P_{max\_sect,j})/r_{out}$, of the probability density function of the variable $P_{max\_sect,j}/r_{out}$ are calculated;
5) A correlation between the mean value, the standard deviation value, and the maximum measured value, $P_{max,p}/r_{out}$ is established by fitting the measured data of the scanned strands

Ref. Franceschini L., Belletti B., Tondolo F., Sanchez J. 2022. Study on the Probability Distribution of Pitting for Naturally Corroded Prestressing Strands Accounting for Surface Defects. Buildings 12(10), Article number 1732

Simplified model for Corroded Prestressing Strands (SCPS): some assumptions about corrosion morphology

SCPS model is an equivalent spring model
based on only one parameter that is the
$\frac{P_{ma\ \_sect,j}}{r_{out}}$

$$\frac{P_{av\_sect,j}}{r_{out}} = 0.378\left(\frac{P_{ma\,x\,\_sect,j}}{r_{out}}\right)^2 + 0.25\frac{P_{ma\ \_sect,j}}{r_{out}}$$

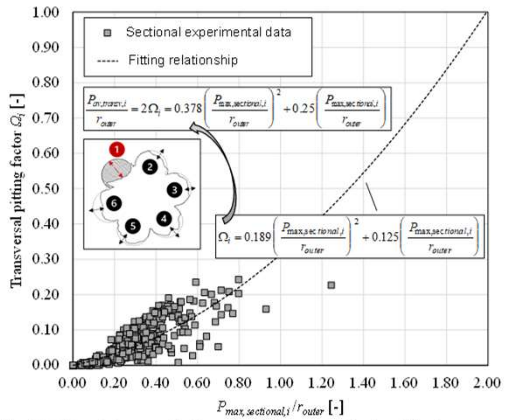

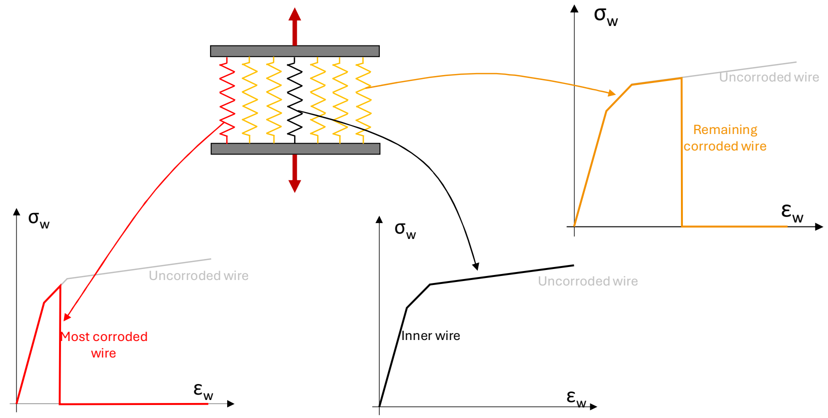

Steps for the probabilistic distribution of the corrosion morphology obtained from the 3D-scan:

6) at the j-th section, the same pit depth for the remaining five outer wires, $P_{av\_sect,j}/r_{out}$, is assumed and calculated as a function of the pith depth of the most corroded wire, $P_{max\_sect,j}/r_{out}$

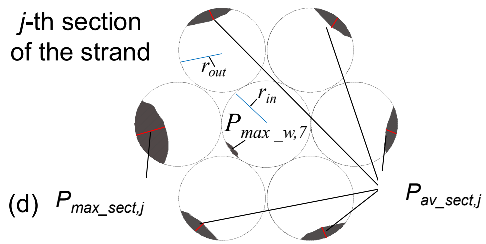

L. Franceschini, B. Belletti, F. Tondolo, and J. Sanchez Montero, “A simplified stress-strain relationship for the mechanical behaviour of corroded prestressing strands: the SCPS-model,” Structural Concrete, vol. 24, no. 1, pp. 189–210, 2022

Simplified model for Corroded Prestressing Strands (SCPS): some assumptions about corrosion morphology

Decay in cross-section area of wire

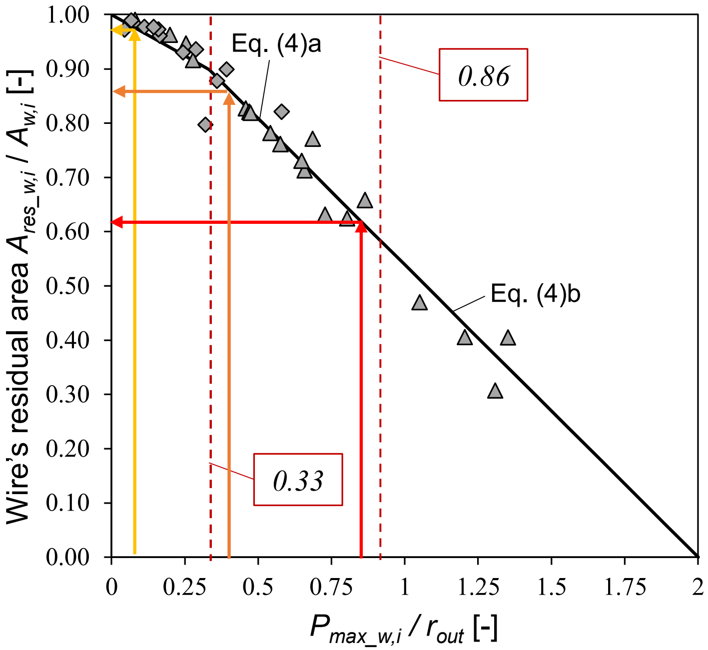

$$\frac{\mu(P_{\max\_sect,j})}{r_{out}} = 0.14$$

$$\frac{\mu(P_{\max\_sect,j})}{r_{out}} = 0.43$$

$$\frac{\mu(P_{\max\_sect,j})}{r_{out}} = 0.82$$

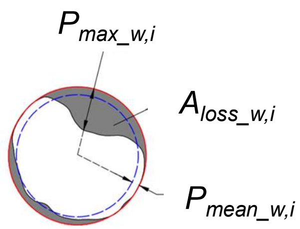

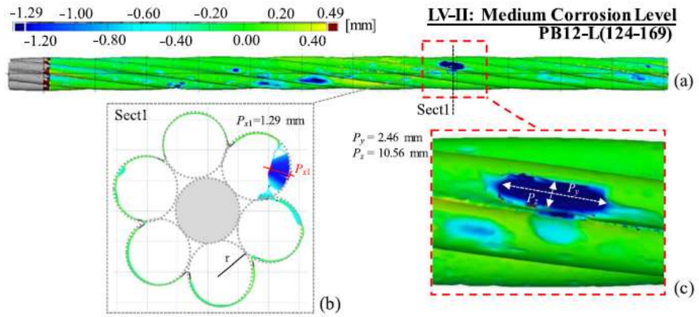

The 3D-scan of the section loss of each wire, $A_{loss\_w,i}$, allows to directly relate the maximum pit depth of each wire, $P_{max\_w,i}$, with the residual cross-sectional area of the corroded wires

$$\frac{A_{res\_w,i}}{A_{w,i}} = \left(1 - 0.33 \cdot \frac{P_{ma\ \_w,i}}{r_{out}}\right) \quad \text{for } \frac{P_{ma\ \_w,i}}{r_{out}} \leq 0.33$$

$$\frac{A_{res\_w,i}}{A_{w,i}} = \left[0.9 - 0.539 \cdot \left(\frac{P_{ma\ \_w,i}}{r_{out}} - 0.33\right)\right] \quad \text{for } \frac{P_{ma\,x\_w,i}}{r_{out}} > 0.33$$

L. Franceschini, B. Belletti, F. Tondolo, and J. Sanchez Montero, "A simplified stress-strain relationship for the mechanical behaviour of corroded prestressing strands: the SCPS-model," Structural Concrete, vol. 24, no. 1, pp. 189–210, 2022

Simplified model for Corroded Prestressing Strands (SCPS): tensile resistance of corroded strands

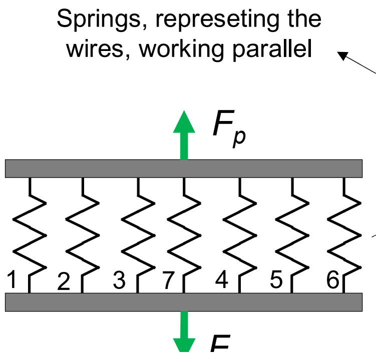

$$\sigma = \begin{cases} E_p \cdot \varepsilon & \varepsilon \le \varepsilon_{pp} \\ f_{pp} + E'_p \cdot (\varepsilon - \varepsilon_{pp}) & \varepsilon_{pp} < \varepsilon \le \varepsilon_{py} \\ f_{pp} + E''_p \cdot (\varepsilon - \varepsilon_{py}) & \varepsilon_{py} < \varepsilon \le \varepsilon_{pu} \end{cases}$$

$$E'_p = \frac{f_{py} - f_{pp}}{\varepsilon_{py} - \varepsilon_{pp}} \qquad E''_p = \frac{f_{pt} - f_{py}}{\varepsilon_{pu} - \varepsilon_{py}}$$

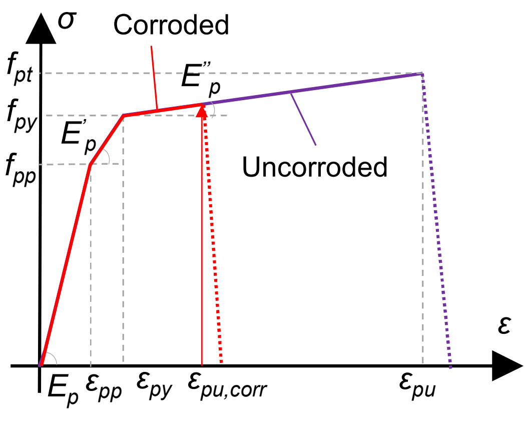

(b)

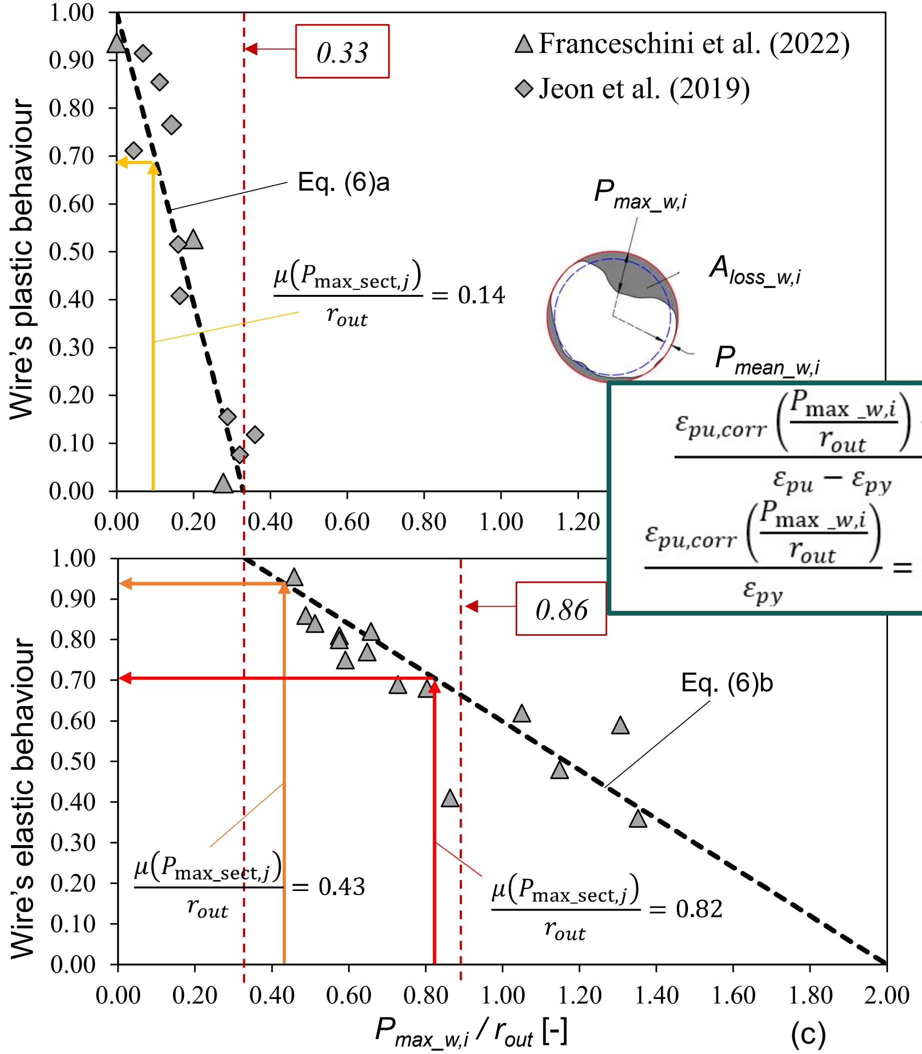

(c)

Ultimate strain of the corroded wire, $\varepsilon_{pu,corr}$

$$\frac{\varepsilon_{pu,corr}\left(\frac{P_{\max\_w,i}}{r_{out}}\right) - \varepsilon_{py}}{\varepsilon_{pu} - \varepsilon_{py}} = 1 - 3.03 \cdot \frac{P_{\max\_w,i}}{r_{out}} \quad \text{for } \frac{P_{\max\_w,i}}{r_{out}} \le 0.33$$

$$\frac{\varepsilon_{pu,corr}\left(\frac{P_{\max\_w,i}}{r_{out}}\right)}{\varepsilon_{py}} = 1 - 0.599 \cdot \left(\frac{P_{\max\_w,i}}{r_{out}} - 0.33\right) \quad \text{for } \frac{P_{\max\_w,i}}{r_{out}} > 0.33$$

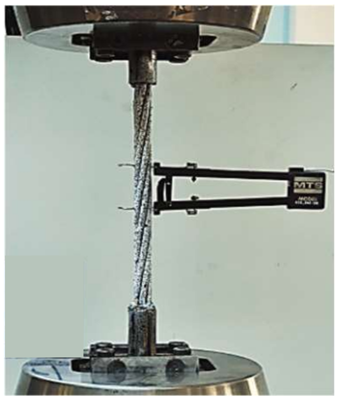

Simplified model for Corroded Prestressing Strands (SCPS): tensile resistance of corroded strands

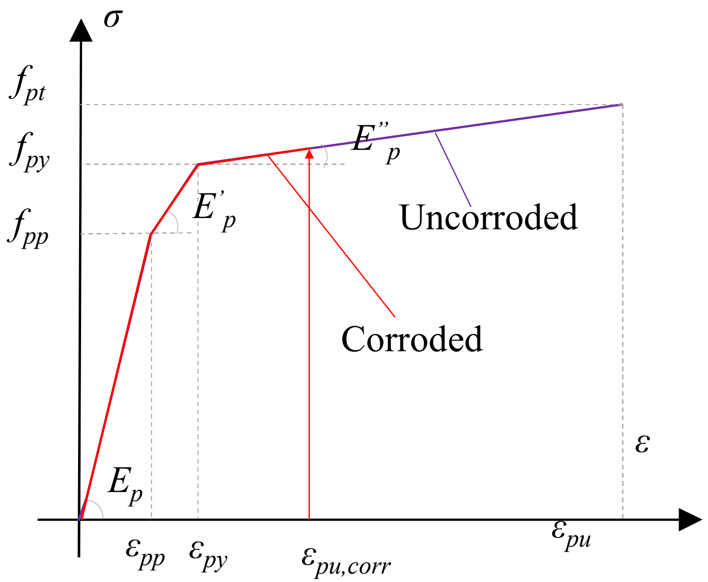

(a)

f_{pp} = 0.7 f_{pt}

f_{py} = 0.882 f_{pt},

while $\varepsilon_{pp} = f_{pp}/E_p$ and ε_{py} = 0.01

Since prestress value ranges around 0.5 – 0.6 f_{pt}, it results that, for pits dept of the wire higher than the value given by the following equation cause a premature and brittle rupture of the wire only due to the applied prestressing force

$$\varepsilon_{pu,corr}\left(\frac{P_{\text{ma}\quad\_w,i}}{r_{out}}\right) = \varepsilon_{p0} \quad \Rightarrow \quad \left[\frac{P_{\text{ma}\quad\_w,j}}{r_{out}}\right]_{p0} \geq \left[0.33 + \frac{1}{0.599}\left(1 - \frac{\varepsilon_{p0}}{\varepsilon_{py}}\right)\right]$$

As the applied prestressing force increases - and consequently as the value of ε_{p0} increases -, as the corrosion level, defined in terms of $P_{max\_w,j}$, that cause premature and brittle wire's rupture decreases.
Therefore, the fragility of PC members is not only related to the corrosion level but also to the value of the prestressing strain applied in strands.

Simplified model for Corroded Prestressing Strands (SCPS): tensile resistance of corroded strands

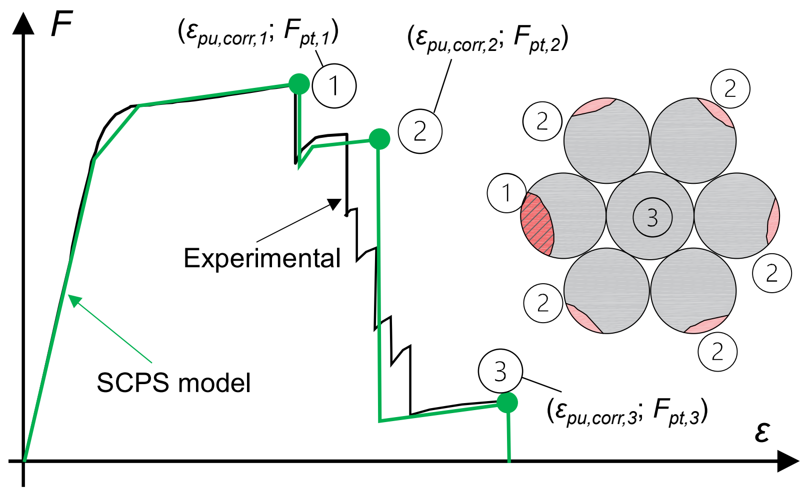

The relation tensile resistance vs strain of the strand, instead of being characterised by 7 softening steps corresponding to the sequential failure of the 7 wires, is characterised by 3 steps corresponding to:

1) The failure of the most corroded wire (point 1),
2) The failure of the remaining five outer wires (point 2),
3) The failure of the inner wire (point 3)

$$F_{pt,1} = \sigma\left(\varepsilon_{pu,corr}\left(\frac{P_{\max\_sect,j}}{r_{out}}\right)\right) \cdot \left[A_{res\_w}\left(\frac{P_{\max\_sect,j}}{r_{out}}\right) + 5A_{res\_w}\left(\frac{P_{av\_sect,j}}{r_{out}}\right) + A_{w,in}\right]$$

$$F_{pt,2} = \sigma\left(\varepsilon_{pu,corr}\left(\frac{P_{av\_sect,j}}{r_{out}}\right)\right) \cdot \left[5A_{res\_w}\left(\frac{P_{av\_sect,j}}{r_{out}}\right) + A_{w,in}\right]$$

$$F_{pt,3} = f_{pt} \cdot A_{w,in}$$

Simplified model for Corroded Prestressing Strands (SCPS): validation

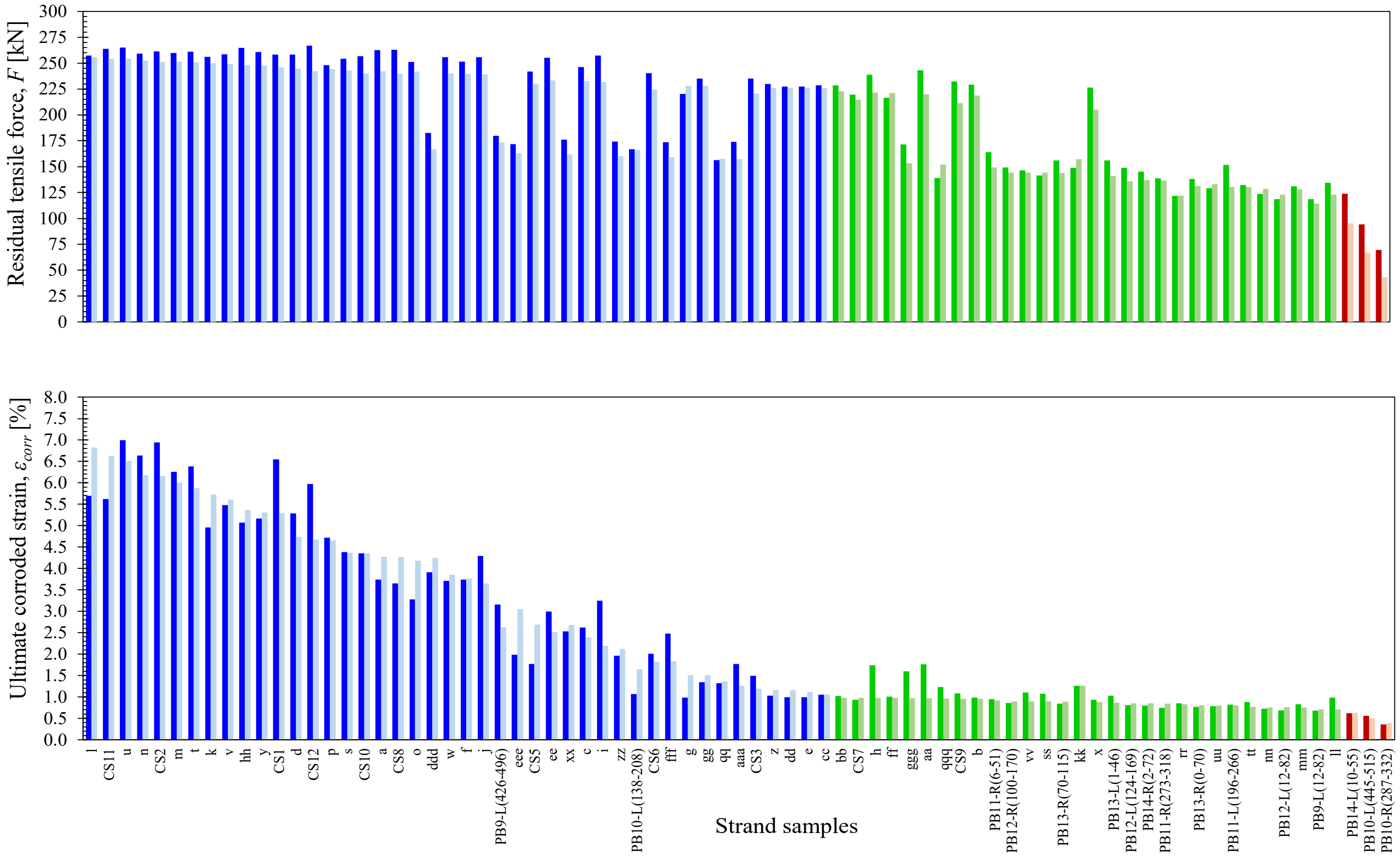

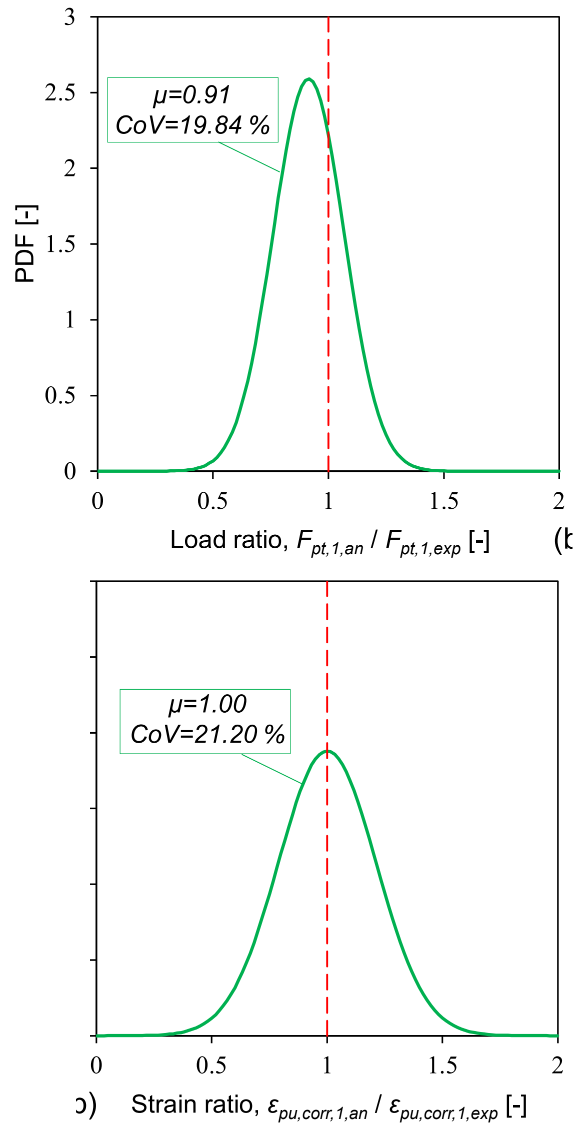

The first approach to define the intensity level, $k_{int,1}$

THE INTENSITY LEVEL, k_{int}

The second approach to define the intensity level, $k_{int,2}$

The first approach to define the intensity level, $k_{int,1}$

- Three different levels of intensity are assumed in correspondence of three different damages that can be qualitatively noted during visual inspections

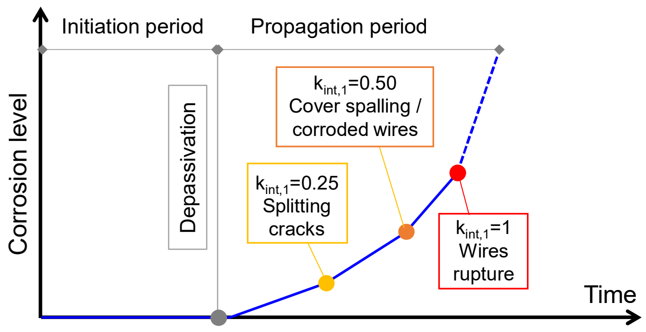

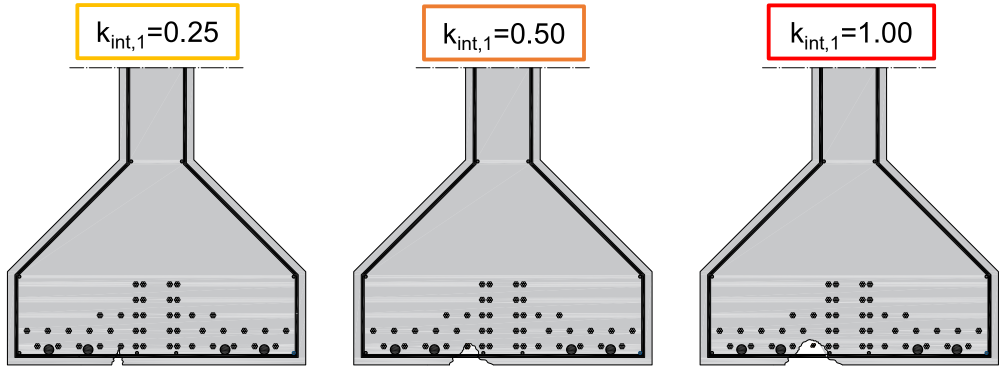

0 - 1: Initiation phase	**1 - 2**: Visible splitting cracks $k_{int,1}$ = 0,25	**2 - 3**: concrete cover spalling and visible section loss in corroded wires $k_{int,1}$ = 0,5	**3 - 4**: 100% cross-section loss of some wires in strands $k_{int,1}$ = 1
			

The second approach to define the intensity level, $k_{int,2}$

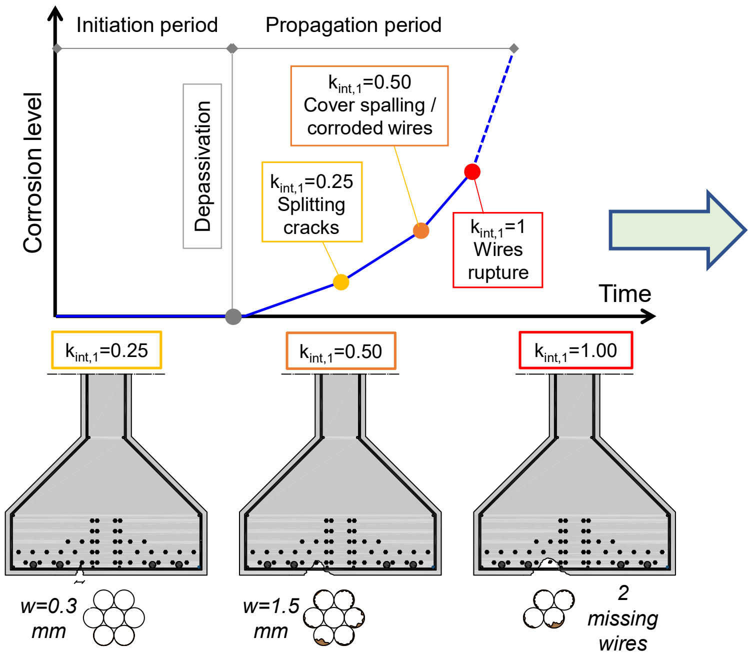

(a)

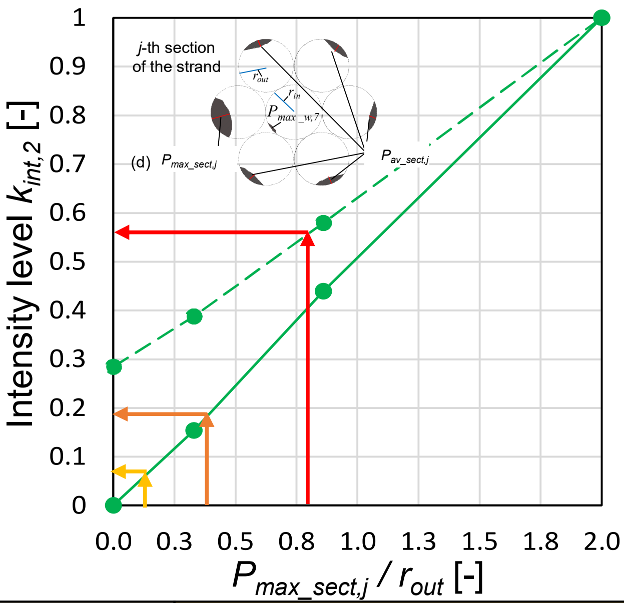

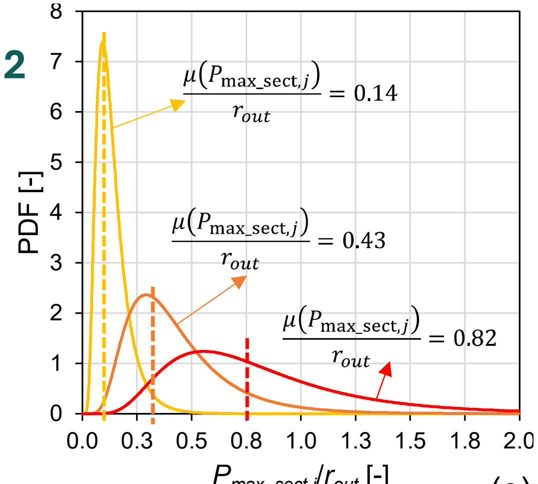

(e)

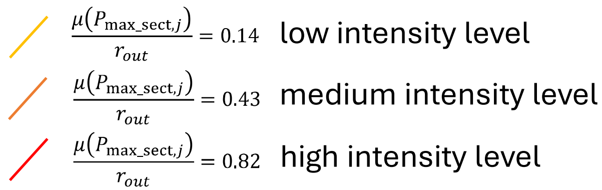

(b)

0 - 1: Initiation phase	**1 - 2**: Visible splitting cracks Assumed value for the example: w = 0.3 mm **A range of value could be selected**	**2 - 3**: concrete cover spalling and visible section loss in corroded wires Assumed value for the example: w = 1.5 mm **A range of value could be selected**	**3 - 4**: 100% cross-section loss of some wires in strands Assumed value for the example: 2 wires having 100 % section loss **selected quite arbitrarily**
			

The second approach to define the intensity level, $k_{int,2}$

For low and medium intensity levels, the relation between corrosion in strands and crack opening width proposed by Ahmed et al. has been modified to be directly implemented in *SCPS* model.

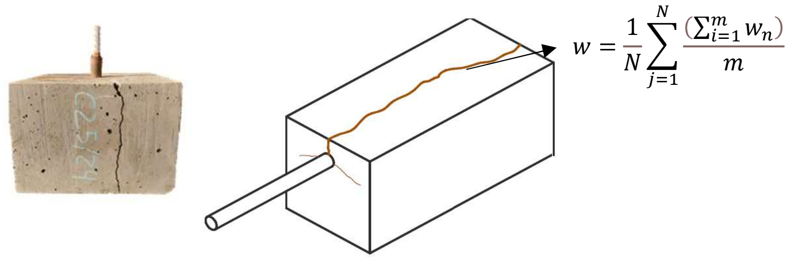

$$w = 0.16\,\frac{e^{\left(\sigma_{p0}/f_{pt}\right)}}{R_{w/c}}\left(P_{sum\_sect,j} - P_0\right)$$

Assumptions: prestress σ_{p0}=0,5 f_{pt}, the water-cement ratio $R_{w/c}$ = *0.5*, the cover-diameter ratio, c/ϕ_p = 3.3

P_0 the sum of the pit depths in external wires corresponding to splitting crack initiation:

$$P_0 = 0.036\,\frac{R_{w/c}}{e^{\left(\sigma_{p0}/f_{pt}\right)}}\left[\frac{c}{\phi_p}\right]^2 + 0.128$$

The sum of the pit depth in external wires, $P_{sum\_sect,j}$, is obtained, according to the *SCPS* model, as given

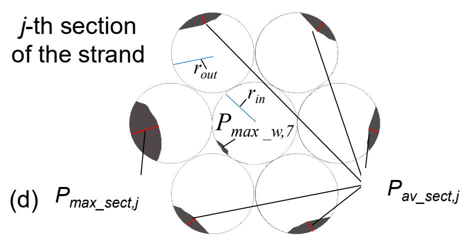

$$P_{sum\_sect,j} = \mu\left(P_{max\_sect,j}\right) + 5\cdot\left[P_{av\_sect,j}\right]_{\left(P_{\mathrm{ma\ x}\_sect,j}\right)}$$

Being:

$$\left[P_{av\_sect,j}\right]_{\left(P_{\mathrm{ma\ x}\_sect,j}\right)} = r_{out}\left[0.378\left(\frac{\left(P_{\mathrm{ma}\ \_sect,j}\right)}{r_{out}}\right)^2 + 0.25\,\frac{\left(P_{\mathrm{ma}\ \_sect,j}\right)}{r_{out}}\right]$$

The second approach to define the intensity level, $k_{int,2}$

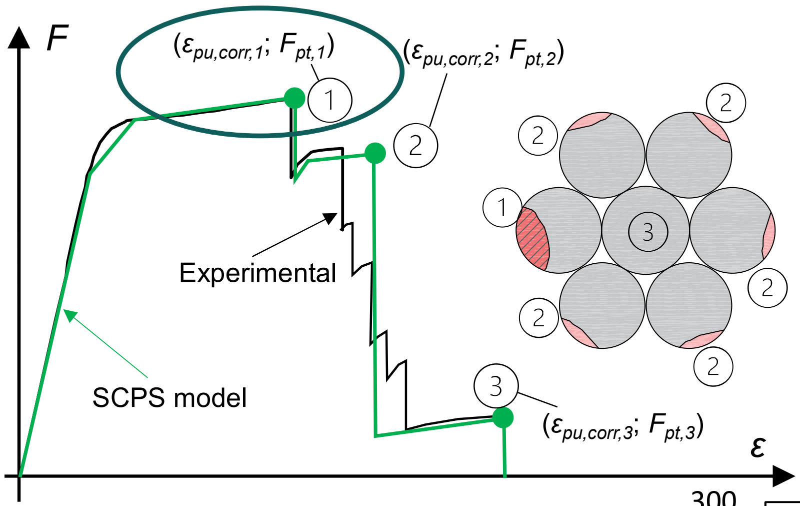

ONLY FOR THIS EXAMPLE!

The assigned values of the intensity level result as follows:

a. visible splitting cracks: $k_{int,2}$ = 0.06
b. concrete cover spalling and visible section loss in corroded wires: $k_{int,2}$ = 0.20
c. 100% cross-section loss of some wires in strands: $k_{int,2}$ = 0.56

$$\boxed{k_{int,2} = 1 - \frac{F_{pt,1}}{F_{pt,0}}}$$

the value of the intensity level, $k_{int,2}$, is adopted to propose a suitable defect-based index for the simplified calculation of the resistant moment of *PC* bridge girders

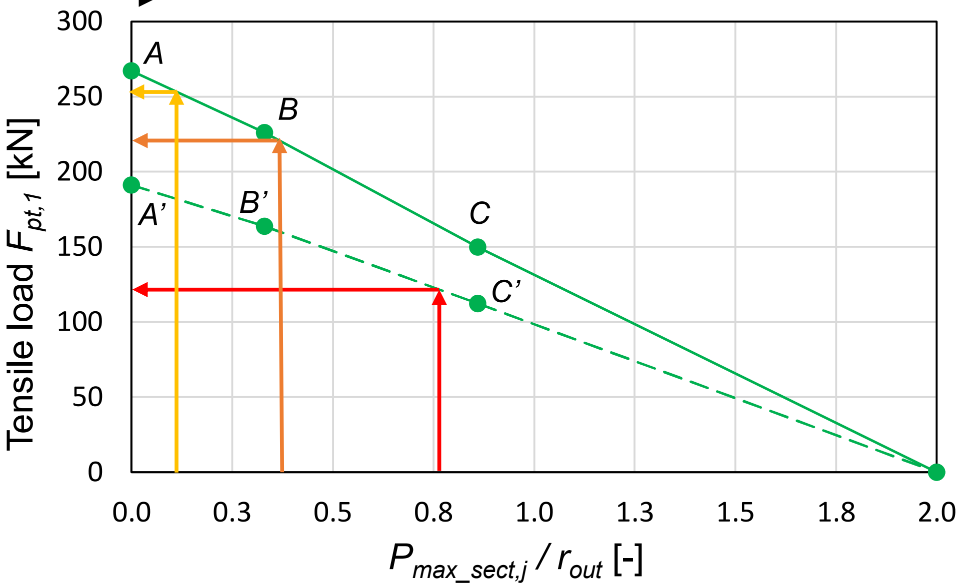

A: $(0;\ F_{pt,0} = f_{pt} \cdot (6 \cdot A_{w,i} + A_{w,in}))$;
A': $(0;\ F_{pt,0} = f_{pt} \cdot (4 \cdot A_{w,i} + A_{w,in}))$;

B: $(0.33;\ F_{pt,1} = f_{py} \cdot (5.68 \cdot A_{w,i} + A_{w,in}))$;
B': $(0.33;\ F_{pt,1} = f_{py} \cdot (3.83 \cdot A_{w,i} + A_{w,in}))$;

C: $(0.86;\ F_{pt,1} = f_{pp} \cdot (4.67 \cdot A_{w,i} + A_{w,in}))$;
C': $(0.86;\ F_{pt,1} = f_{pp} \cdot (3.24 \cdot A_{w,i} + A_{w,in}))$;

$$\frac{\mu(P_{\max\_sect,j})}{r_{out}} = 0.14$$

$$\frac{\mu(P_{\max\_sect,j})}{r_{out}} = 0.43$$

$$\frac{\mu(P_{\max\_sect,j})}{r_{out}} = 0.82$$

THE EXTENSION LEVEL, k_{ext}

The approach to define the extension level, k_{ext}

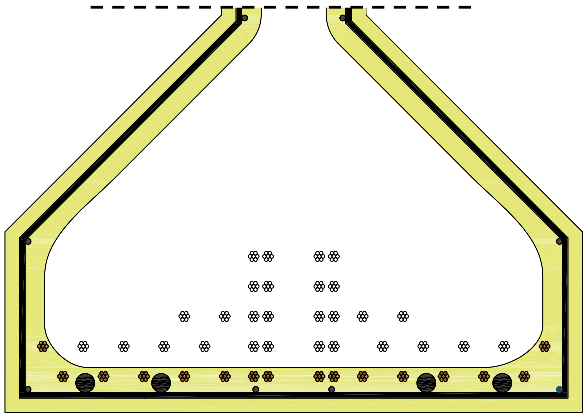

corroded strands /
external strands

k_{ext}	A-A	B-B
25%	3/12	4/16
50%	6/12	8/16
100%	12/12	16/16

Since in this paper the capacity of the analysed prestressed beam is correlated to the damage detected via visual inspection, no assumptions about the corrosion of internal layers are made. Therefore, internal strands are considered uncorroded.

Consequently, the extension levels of corrosion are established based on the ratio between the corroded and "visible" strands to the total number of external strands.

PROBABILISTIC ASSESSMENT OF THE FLEXURAL CAPACITY OF THE PC GIRDER

Probabilistic assessment of the flexural capacity of the PC girder

FLOW-CHART

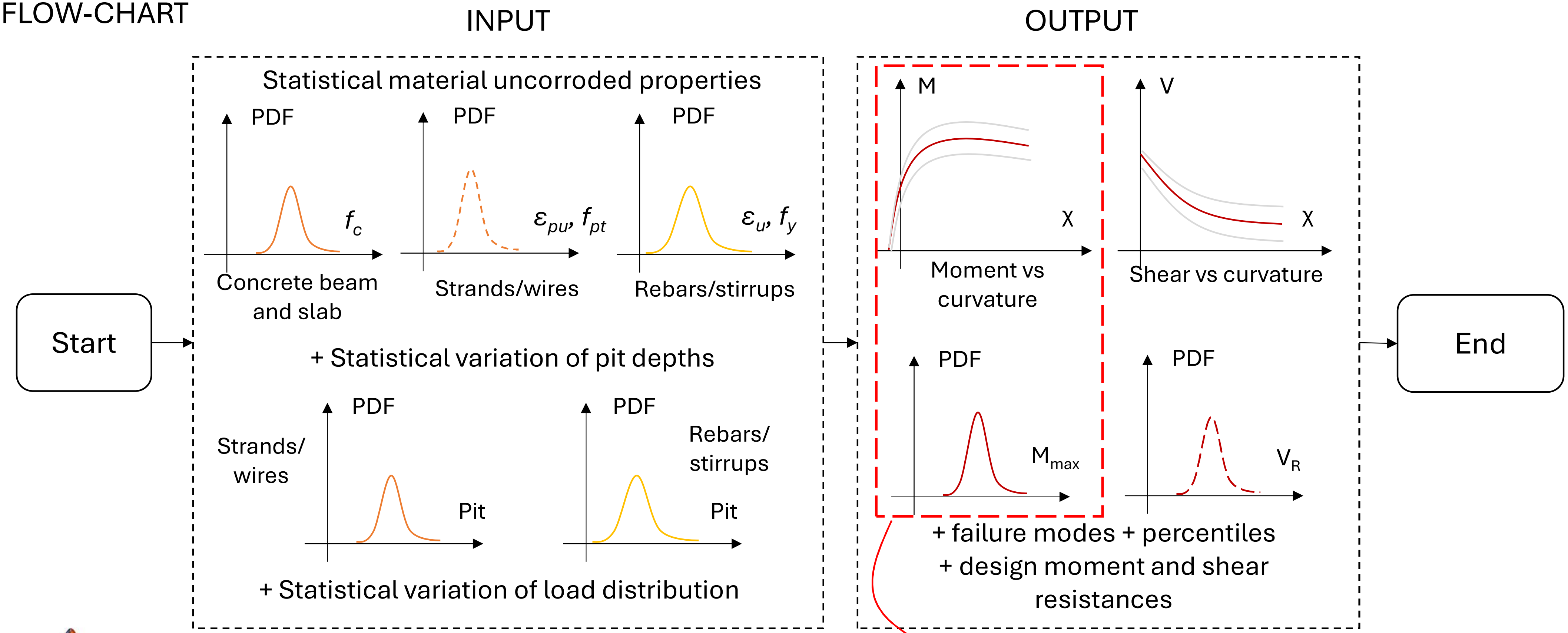

Focus of the current study: assessment of the flexural resistance of the PC girder

Results: Flexural Resistance vs Corrosion Scenarios

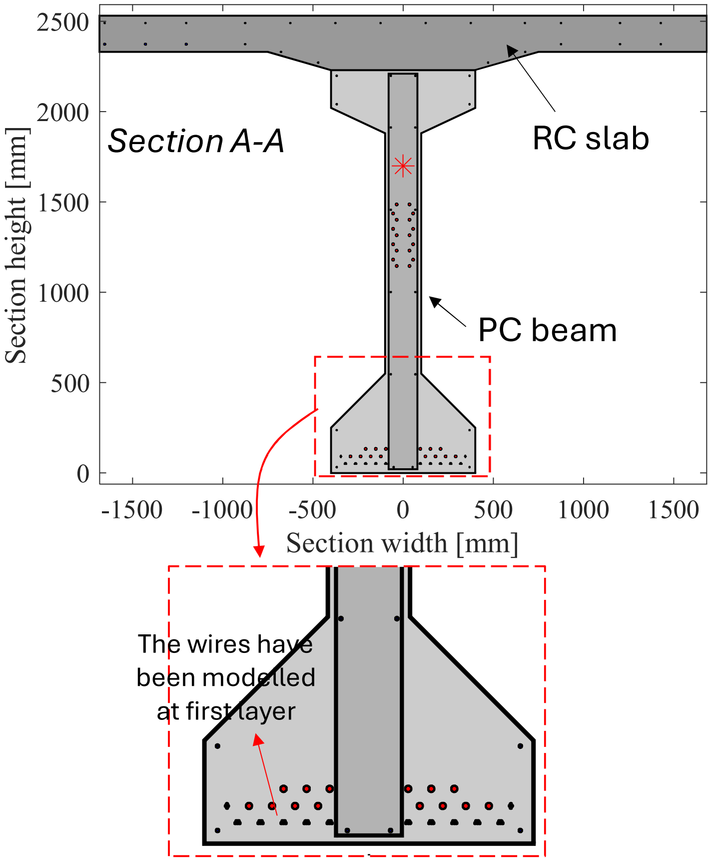

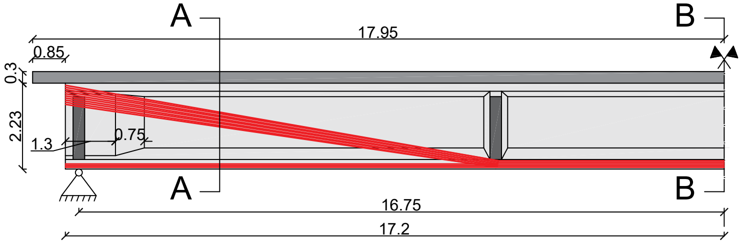

- Flexural resistance in terms of moment vs curvature.
- Degraded strands at bottom flange of the PC beam.
- Curvature-controlled diagram
- Decay of the prestressing force is assumed proportional to the cross-section loss of the strand

$$N_{p,0,corr} = \left(A_{res\_sect,j}/A_{sect,j}\right) \cdot N_{p,0}$$

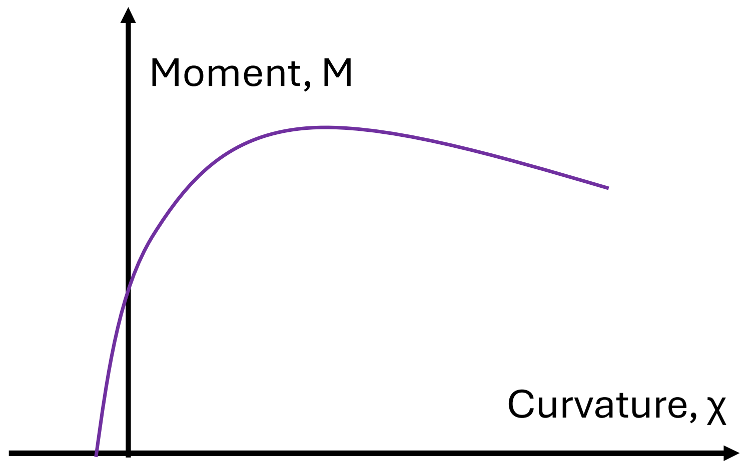

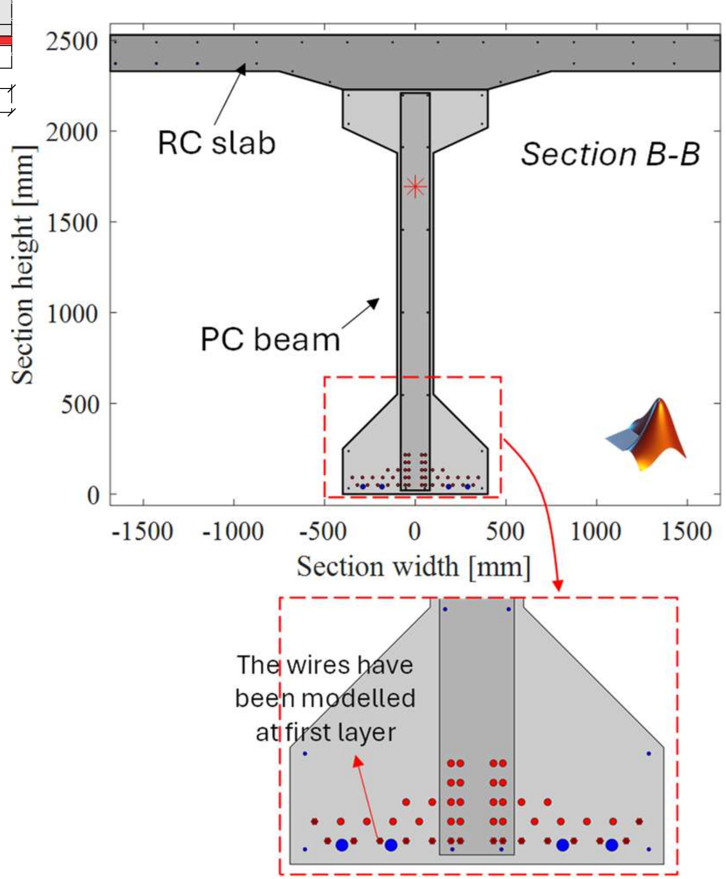

Results: Flexural Resistance vs Corrosion Scenarios

Decay of the flexural resistance vs corrosion

Uncorroded

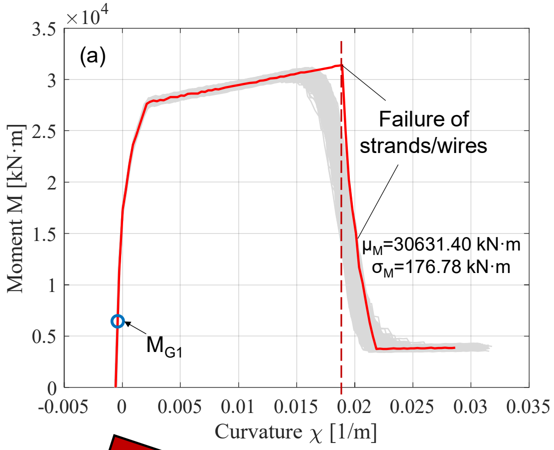

K_{ext}=1, $K_{int,1}$ = 0.25

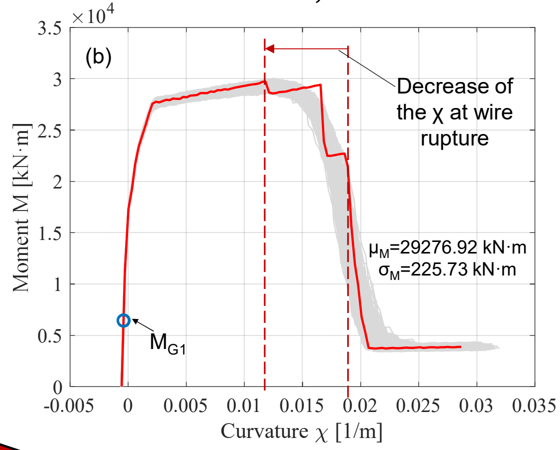

Section B-B

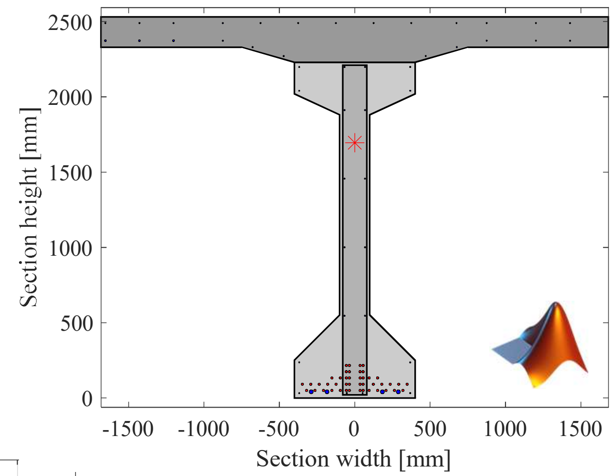

K_{ext}=1, $K_{int,1}$ = 0.50

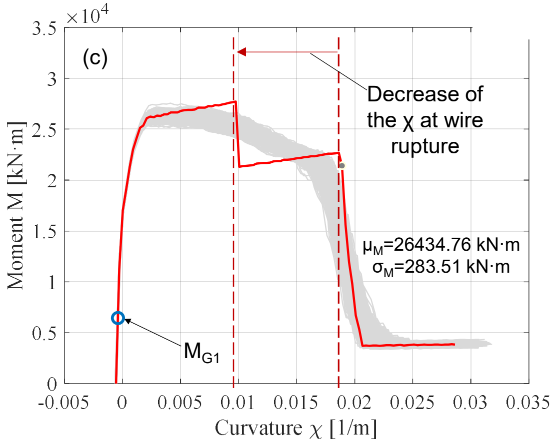

K_{ext}=1, $K_{int,1}$ = 1.00

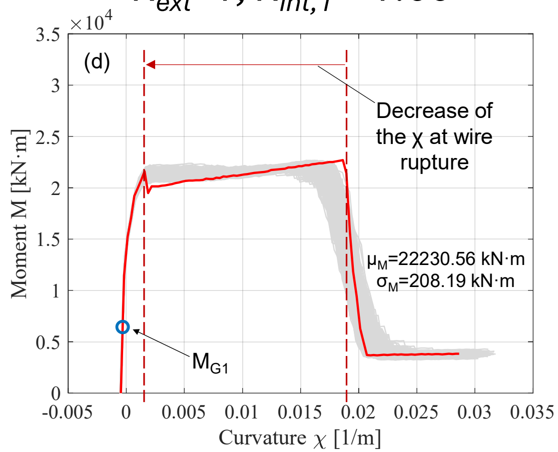

- *INCREASING CORROSION INTENSITY*
- *EXAMPLE of SECTION B-B*

Results: Flexural Resistance vs Corrosion Scenarios

Decay of the flexural resistance vs corrosion

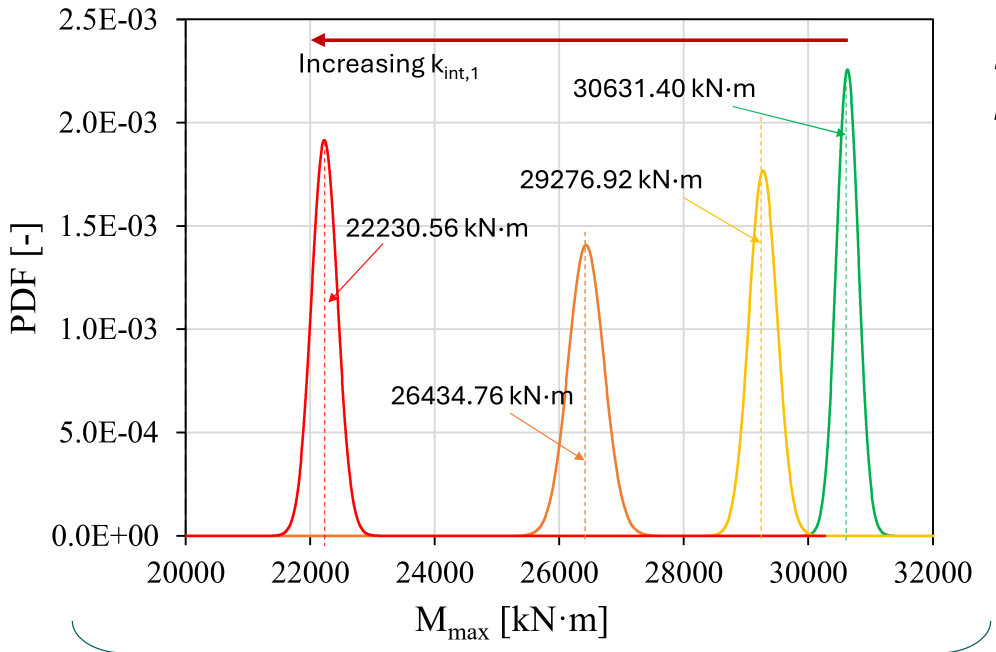

Decay of the maximum moment resistance

Increasing dispersion in the moment resistance

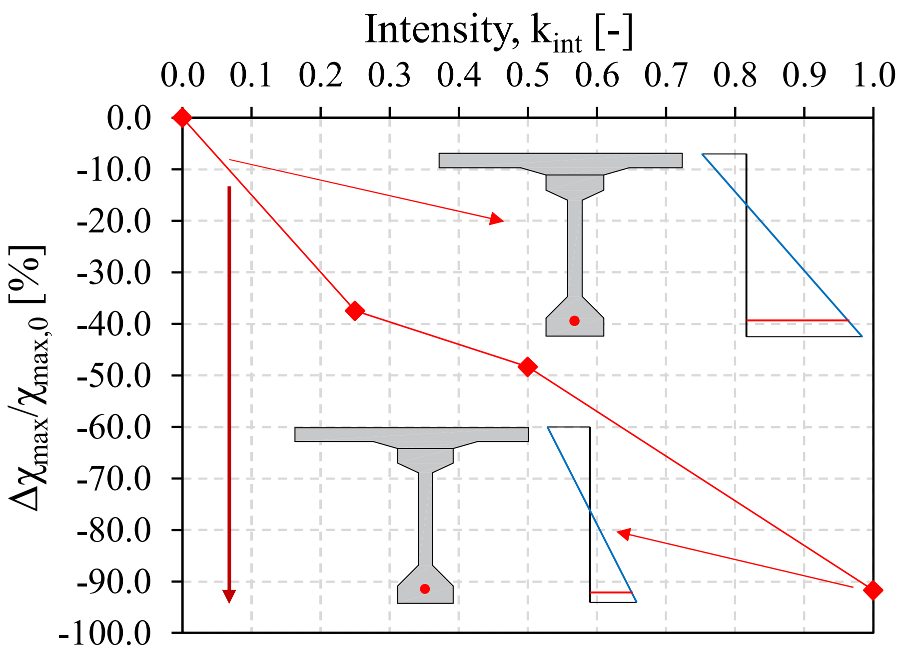

Decay of the curvature at maximum moment resistance

The design value of resistant moment, M_{Rd}, is estimated by intersecting the related cumulative distribution functions (*CDF*) with percentiles calculated by assuming a Generalised Extreme Value (GEV) distribution, a consequence class 3, a target reliability index is equal to 3.7 and - for a reference period of 1 year - a sensitivity factors equal to 0.7

Results: Flexural Resistance vs Corrosion Scenarios

Estimation of the design resistant moment M_{Rd}

Section B-B

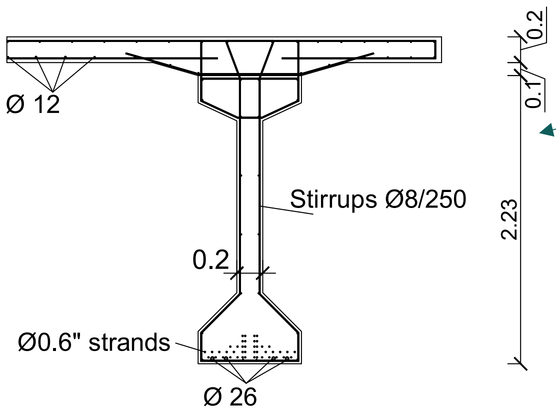

Section A-A

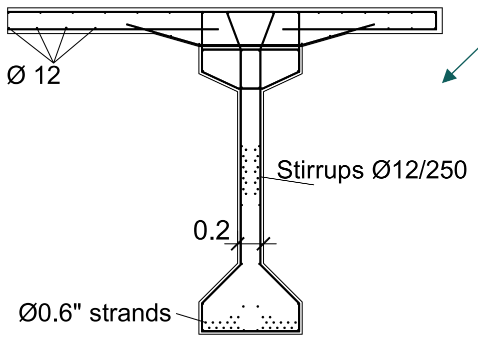

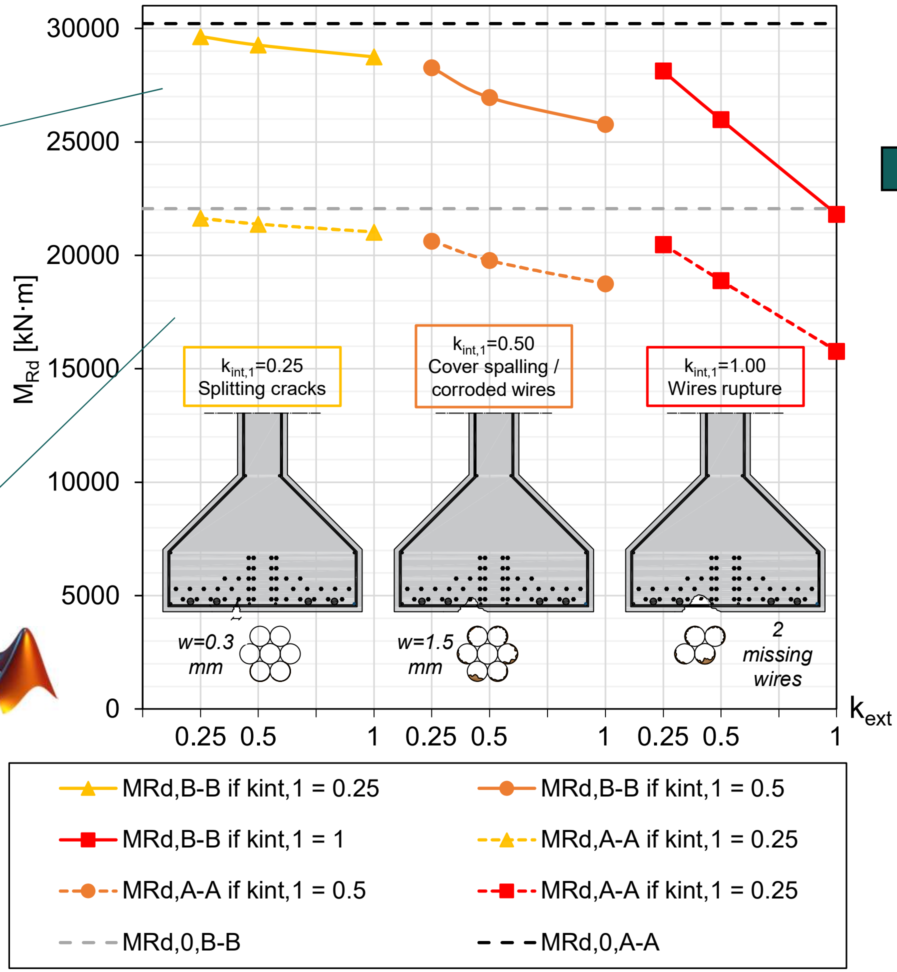

Observations:

- Decay of the resistant moment till 30 %
- Decrease in the sectional ductility

dependency of the decay of the design value of the resistant moment on the intensity and extension levels of corrosion observed during visual in-situ inspections

Required a proposal for a Defect-based index for a simplified calculation of the resistant moment based on a <u>QUANTITATIVE</u> evaluation of the intensity index

!

DEFECT-BASED INDEX TO CALCULATE THE RESISTANT MOMENT

Defect-Based Index to calculate the Resistant Moment

Simplified calculation of the resistant moment

PC girder with strands' and reinforcement internal level arms

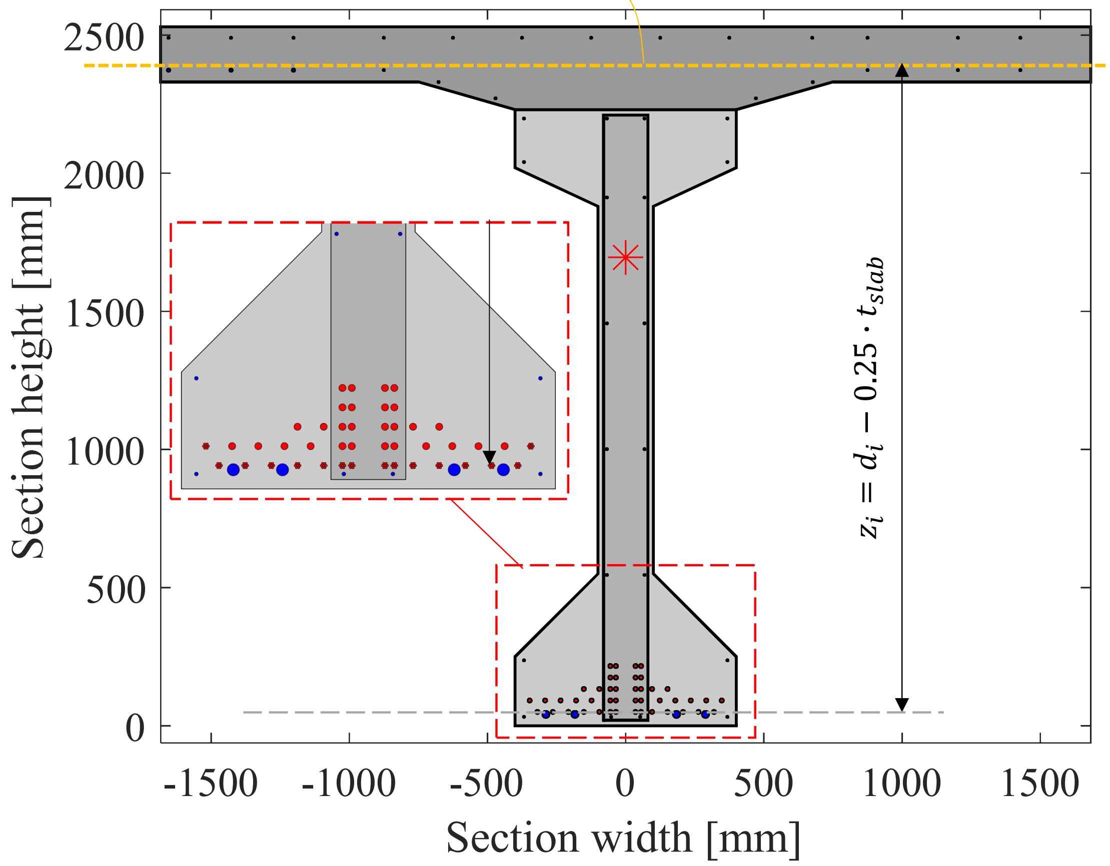

Calculation of the Resistant Moment M_R

- N: total number of prestressing strands
- N_{ext}: total number of external prestressing strands
- Nb: total number of mild rebars

Contribution of inner strands' layers unaffected by corrosion

Contribution of mild steel bars

$$M_R = \sum_{i=1}^{N-N_{ext}} M_{Rp,i} + \sum_{i=1}^{N_{ext}} M_{Rp,i} + \sum_{i=1}^{N_b} M_{Rb,i}$$

Proposed defect-based index adopted to calculate the resistant moment

$$\sum_{i=1}^{N_{ext}} M_{Rp,i} = \boxed{\left(1 - k_{int,2} \cdot k_{ext}\right)} \cdot \boxed{\sum_{i=1}^{N_{ext}} \left(F_{pt,0} \cdot z_i\right)}$$

Uncorroded moment contribution

Contribution of the strands at the first layer affected by corrosion

Defect-Based Index to calculate the Resistant Moment

Simplified calculation of the resistant moment

Proposal of a Defect-Based Index for a simplified calculation of the resistant moment

$$\sum_{i=1}^{N_{ext}} M_{Rp,i} = \boxed{\left(1 - k_{int,2} \cdot k_{ext}\right)} \cdot \sum_{i=1}^{N_{ext}} \left(F_{pt,0} \cdot z_i\right)$$

Proposed defect-based index adopted to calculate the resistant moment

!

$$k_{int,2} = 1 - \frac{F_{pt,1}}{F_{pt,0}}$$

Tensile resistance of the corroded strand

Tensile resistance of the uncorroded strand

NEW INTENSITY INDEX

Decay of the tensile resistance of corroded strands

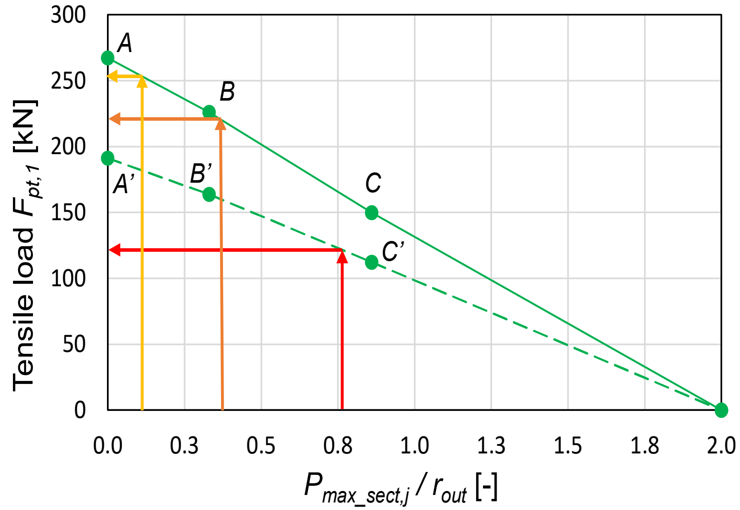

A: $(0; F_{pt,0} = f_{pt} \cdot (6 \cdot A_{w,i} + A_{w,in}))$;
A': $(0; F_{pt,0} = f_{pt} \cdot (4 \cdot A_{w,i} + A_{w,in}))$;

B: $(0.33; F_{pt,1} = f_{py} \cdot (5.68 \cdot A_{w,i} + A_{w,in}))$;
B': $(0.33; F_{pt,1} = f_{py} \cdot (3.83 \cdot A_{w,i} + A_{w,in}))$;

C: $(0.86; F_{pt,1} = f_{pp} \cdot (4.67 \cdot A_{w,i} + A_{w,in}))$;
C': $(0.86; F_{pt,1} = f_{pp} \cdot (3.24 \cdot A_{w,i} + A_{w,in}))$;

$$\frac{\mu(P_{\max\_sect,j})}{r_{out}} = 0.14$$

$$\frac{\mu(P_{\max\_sect,j})}{r_{out}} = 0.43$$

$$\frac{\mu(P_{\max\_sect,j})}{r_{out}} = 0.82$$

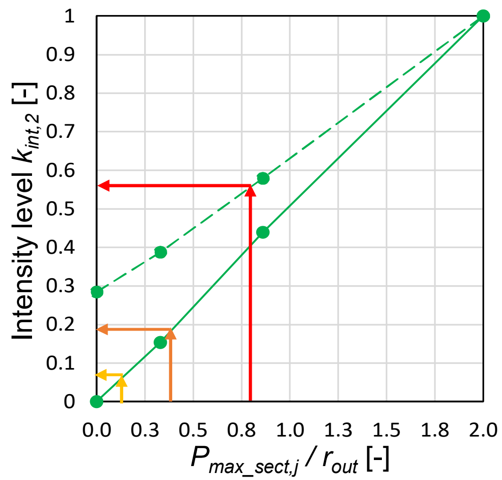

<u>QUANTITATIVE</u> evaluation of the intensity index

Defect-Based Index to calculate the Resistant Moment

Comparisons with the probabilistic results

Section A-A

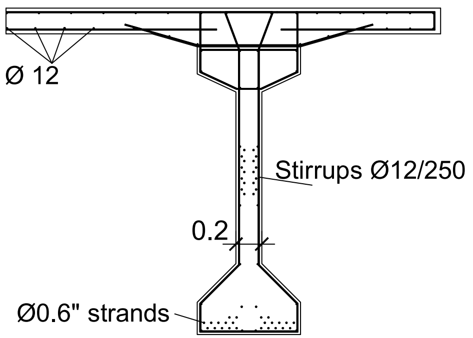

Calculation of the Resistant Moment M_R

$$M_R = \sum_{i=1}^{N-N_{ext}} M_{Rp,i} + \sum_{i=1}^{N_{ext}} M_{Rp,i} + \sum_{i=1}^{N_b} M_{Rb,i}$$

Section B-B

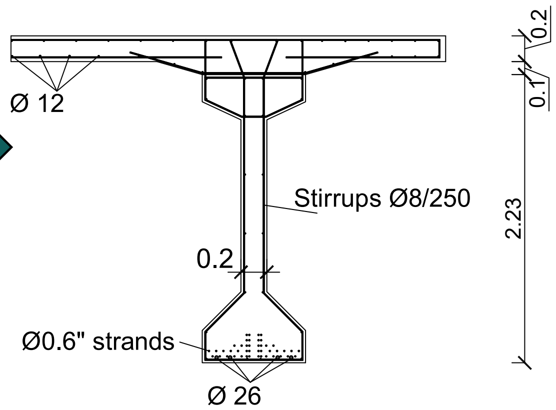

Theoretical/Numerical ratio of resistant moment

$$R_M = \frac{M_{R,theo}}{\mu M_R}$$

Average of the mean resistant moment calculated from the probabilistic assessment for each scenario

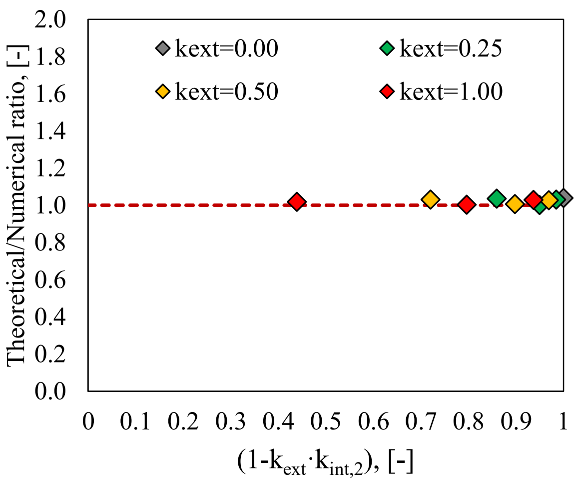

Section	Average [-]	St. Dev. [-]	CoV [%]
A-A	1.02	0.014	1.37
B-B	0.98	0.031	3.20

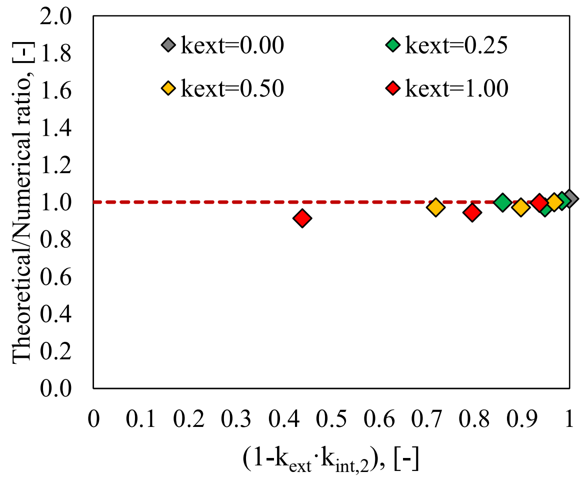

CONCLUSIONS, FUTURE RESEARCH AND PERSPECTIVES

Source of uncertainties must be recognized in the path

In-situ Inspection

- The superficial defect (ex crack opening) can be measured with different tools having different tolerances and levels of accuracy
- The crack opening values adopted to describe different propagation phases need a statistical distribution, not considered in this example

0 - 1: Initiation phase	**1 - 2**: Visible splitting cracks Assumed value for the example: w = 0.3 mm **A range of value could be selected**	**2 - 3**: concrete cover spalling and visible section loss in corroded wires Assumed value for the example: w = 1.5 mm **A range of value could be selected**	**3 - 4**: 100% cross-section loss of some wires in strands Assumed value for the example: 2 wires having 100 % section loss **selected quite arbitrarily**
			

- The geometrical uncertainties,
- The model uncertainties (for example to move from crack opening to pit depth),
- The model uncertainties were considered in previous studies to calibrate partial safety factors for corroded strands, but for a more comprehensive evaluation of all the involved uncertainties, additional studies are required.

$$\boxed{f_{pu,corr,des} = \frac{f_{pu,corr,an}}{\gamma_{m,corr}}}$$

$$\gamma_{m,corr} = \frac{\exp(-1.645V_s)}{\boxed{\mu_{\text{mod}}}\mu_a\mu_{\vartheta R}\cdot\exp\left(-\alpha\beta_{target}\sqrt{\boxed{V_{\text{mod}}^2}+V_a^2+V_s^2+V_{\vartheta R}^2}\right)}$$

1 2 3 4 5 6

μ_{mod} and V_{mod} stand, respectively, for the mean value and the coefficient of variation of **the uncertainty related to the analytical predictions obtained by using the SCPS-model**.

Conclusions, Future Research and Perspectives

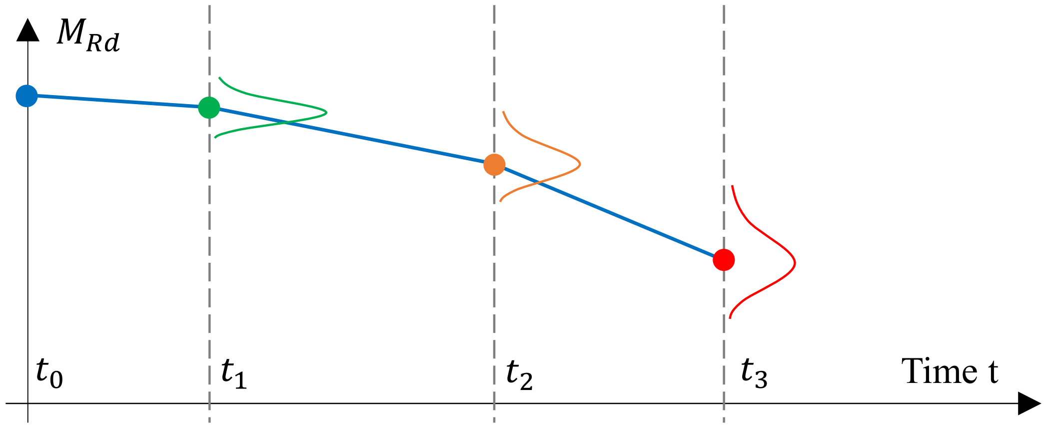

FUTURE RESEARCH, PERSPECTIVES:

- To calibrate models, **DATA** from existing structures, are needed.
- Co-operation between universities, engineering associations, stockholders, etc. is needed to validate models that are recognized suitable for the assessment of corroded existing structures.

Thank you for the attention!

Workshop History (since 2019)

2019 Workshop Parma

- 15 papers
- 3 KN Speakers
- All participants were European

2020 Workshop Online

- 18 papers
- 10 KN Speakers
- 15 countries worldwide
- 47 National Participants, 21 International

2021 Workshop Online

- 43 papers
- 15 KN Speakers
- 16 countries worldwide
- 34 National Participants, 41 International

2023 Workshop Parma

- 77 papers
- 18 KN Speakers
- 18 countries worldwide
- 46 National Participants, 32 International

2025 fibCACRCS Lecco

- 71 papers
- 22 KN Speakers
- 19 countries worldwide
- 62 National Participants, 40 International